REPORT No. 508

ANALYSIS OF 2-SPAR CANTILEVER WINGS WITH SPECIAL REFERENCE TO TORSION AND LOAD TRANSFERENCE

By PAUL KUHN

SUMMARY

This paper deals with the analysis of 2-spar cantilever wings in torsion, taking cognizance of the fact that the spars are not independent, but are interconnected by ribs and other structural members. The principles of interaction are briefly explained, showing that the mutual relief action occurring depends on the "pure torsional stiffness" of the wing cross section. Various practical methods of analysis are outlined. The "Friedrichs-von Kármán equations" are shown to require the least amount of labor. These equations were originally derived for wings that owe their torsional stiffness to the individual torsional stiffnesses of the spars; it is shown, however, that the equations apply also to wings in which the torsional stiffness is due to drag bracing—wires or stressed skin—arranged in two planes.

Numerical examples by the several methods of analysis are given and the agreement between the calculation and experiment is shown. In the case of a trussed-spar structure the results are practically equivalent to the results of standard least-work calculations which treat the structure as a pin-jointed space framework, but they can be obtained with so much less labor that the analysis may be made as a routine design procedure.

INTRODUCTION

The forces acting on a cantilever wing produce, in general, bending and torsion of the wing frame, the term "wing frame" being used here to denote the combination of spars and such structural elements as ribs and drag wires which connect the spars and contribute to the structural strength.

The present investigation deals with the transference of forces between the spars due to the connecting elements and is concerned with methods of analysis suitable for practical use. The work was confined to the problem of cantilever 2-spar wings chiefly because the interaction effect is relatively more important for this type of wing than for any other type. A survey of the literature showed that the first article discussing interaction effect was published in Germany in 1918 and has been available in an English translation (reference 1) since 1923. For wing frames without drag bracing a very convenient method has been developed by Friedrichs and von Kármán (reference 2). As the Friedrichs-von Kármán formulas have apparently never been published in English, their derivation is given. The method is then extended to cover other cases of 2-spar construction, and the available experimental evidence is analyzed by this method. For comparison, a conventional method of analysis is used in some cases, and it is shown that the labor of computation by this method may be reduced without appreciable error by assuming that only one or two ribs are active in transferring the load. The simplified conventional method gives good approximations for the bending moments in the spars.

WING FRAMES WITH DRAG BRACING IN A SINGLE PLANE AND WITH PARALLEL SPARS

WING FRAMES WITH INDEPENDENT SPARS

Let us consider briefly the action of a 2-spar wing frame conforming to the usual assumption that the ribs are simply supported at the spars, so that there is no interaction between the spars. The load P (fig. 1) is distributed between the two spars according to the position of its point of application. In general, the deflections of the spars resulting from the components P_F and P_R will differ, resulting in a twist of the wing. There is, however, one point of the section at which P may be applied without causing a twist; this point is called the "elastic center" of the section, and its position is given approximately by the condition

$$a_0 : b_0 = E_R I_R : E_F I_F \qquad (1)$$

where E is the modulus of elasticity, I the moment of inertia, and the subscripts R and F refer to rear and front, respectively.

The locus of the elastic centers of a wing is called the "elastic axis" or the "axis of twist." This axis may usually be approximated by a straight line; a large deviation from the straight line may occur, but for the present purpose the influence of such a deviation is small if it occurs only close to the root and will be neglected.

For purposes of analysis it is convenient to replace a load P in an arbitrary position by a direct bending

load P at the elastic center and a couple Pe, where e is the distance between the point of application of P and the elastic center. The total stresses will be obtained by superposing the stresses due to the bending load and the stresses due to the torque; only the analysis of the stresses due to torque will be dealt with in the following investigation.

In figure 2 is shown a 2-spar system with a pure torque acting on it, exerted by equal and opposite

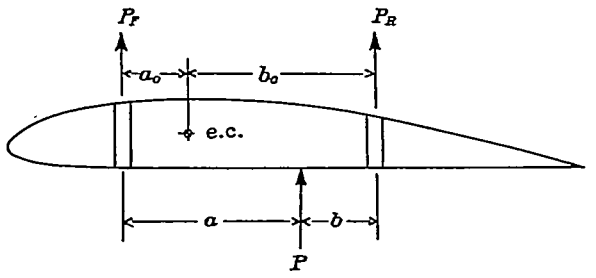

FIGURE 1.—Two-spar wing section.

uniform running loads on the two spars. The torque $T=wLb$ is taken up entirely by bending of the spars, and if the cross sections of the spars are constant, the angle of twist at the tip in radians is

$$\theta=\frac{wL^4}{8bA_0} \tag{2}$$

where A_0 is defined by $\frac{1}{A_0}=\frac{1}{A_F}+\frac{1}{A_R}$, $A_F=EI_F$, and $A_R=EI_R$.

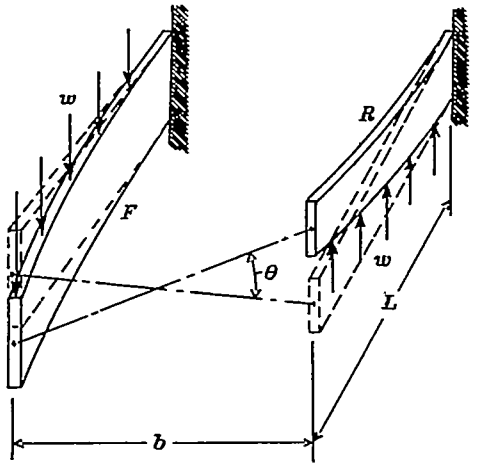

FIGURE 2.—Deformation of 2-spar wing without interaction.

WING FRAMES WITH ONE RIB

Principles of interaction.—The elastic axis of a wing frame can be computed for most types of 2-spar construction; consequently, as indicated in the paragraphs on wings with independent spars, it will always be assumed that the elastic axis has been found and that the load has been resolved into a bending load and a torque. The loading condition investigated will be a pure torque; i.e., equal and opposite loads on front and rear spars at any station. The general case of arbitrary loadings on front and rear spars will, however, be briefly discussed in a later section.

A wing with independent spars having been considered, the next step will be to consider a wing frame consisting of two spars connected by a rib at the tip. It may be well to emphasize here that throughout this report the term "rib" is used to denote a rib specially designed for the purpose of transferring loads from one spar to another. It will be assumed that such ribs are

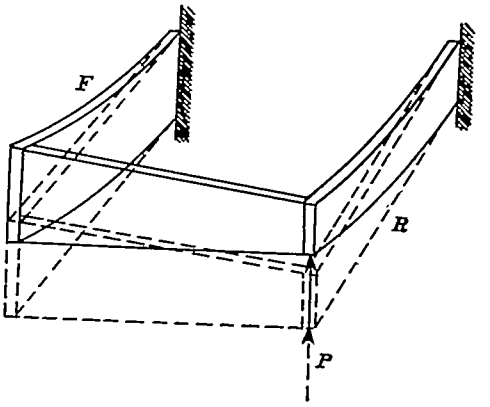

FIGURE 3.—Deformation of wing frame with spars of infinite torsional stiffness.

rigid against bending in their own plane, but have negligible torsional stiffness against warping out of their plane. Checks of existing designs have shown that this assumption can be fulfilled with the practical accuracy required.

Figures 3 and 4 show a wing frame consisting of a deep, stiff front spar and a shallow, flexible rear spar. The load may consist of two equal and opposite forces

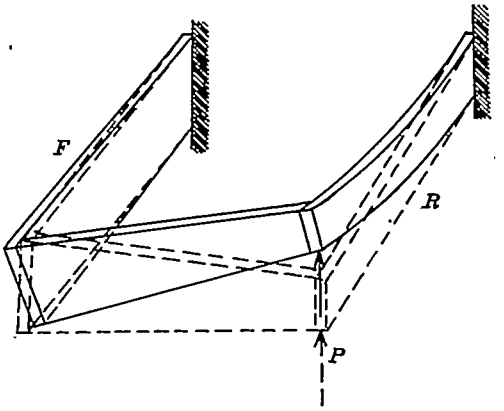

FIGURE 4.—Deformation of wing frame with spars of zero torsional stiffness.

P applied at the tip, but only one of them has been indicated since this is sufficient to explain the action.

Figure 3 shows a state of deformation that might be predicted after very superficial inspection. The front spar has been forced by the tip rib to deflect the same amount as the rear spar. For any number of ribs, the condition that the front-spar deflection equals the rear-spar deflection at each rib would furnish sufficient equations to solve the indeterminate structure. This consideration was the basis for proposed analytical

(reference 3) and graphical (reference 4) methods of investigating wing frames.

A little reflection, however, shows that this assumption is unconservative. The assumed resultant action would occur only if the torsional stiffness of the spars were infinite. Actually, a number of spar sections in common use tend to approach the opposite extreme of negligible torsional stiffness. Figure 4 shows the resultant deformation of such a wing frame. *Without torsional stiffness, the front spar simply twists without offering any aid to the loaded rear spar.*

Calculation of relief moment.—Figure 5 shows a wing frame consisting of two parallel spars connected by a rib at the tip. For convenience, the cross sections are at first assumed constant.

The load is a torque, exerted by equal and opposite uniform running loads on each spar. The structure is made determinate by cutting the rib and introducing as unknowns the shear force X and the bending moment Y in the rib.

The external loads cause vertical displacements of the two edges of the cut in the rib, and the two unknowns are calculated from the two conditions of continuity: The relative angular displacement of the two edges must be zero, and the relative vertical displacement of the two edges of the cut must be zero. The first condition is fulfilled if the cut is made at such a location that

$$\frac{a}{B_F}=\frac{b-a}{B_R} \tag{3}$$

where $B_F=GJ_F$ is the torsional stiffness of the front spar. (See appendix A.) If the cut is made at this point, the bending moment Y is zero, leaving the shear force X as the only unknown, to be calculated by using the second condition of continuity.

The relative vertical displacement at the cut due to the external forces is

$$y_e=\frac{wL^4}{8A_0} \tag{4}$$

where A_0 has the same meaning as in equation (2). The relative vertical displacement due to X consists of two parts, a direct bending deflection of the spars and a vertical displacement of the cut due to twist of the spars.

$$y_X=\frac{XL^3}{3A_0}+\frac{XLb^2}{B_0} \tag{5}$$

where $B_0=B_F+B_R$. (Formulas for calculating B are given in appendix A.) Equation (5) holds whether or not the front and rear spars are alike.

The second condition of continuity requires that $y_e=y_X$, which gives

$$X=\frac{3wL}{8\left(1+3\frac{b^2A_0}{L^2B_0}\right)} \tag{6}$$

The bending moment in the spar without interaction is equal at any point to the externally applied moment $M_e=\frac{wx^2}{2}$. With the rib intact, the bending moment M at any point x is obtained by subtracting from M_e the relief moment $m=xX$ due to the action of the shearing force X in the rib.

Although all the foregoing calculations were made under the assumption of constant-spar cross sections, the methods used can be extended without difficulty to the case of variable cross sections and any arbitrary loading condition. The only difference is that some additional labor will be required to calculate the deflections by integration; ordinarily, this will be an approximate numerical integration or perhaps a graphical one.

Estimate of torsional stiffness required.—Formula (6) shows that the relief moment depends on the quantity $\frac{b^2A_0}{L^2B_0}$. Since the bending stiffness and spar

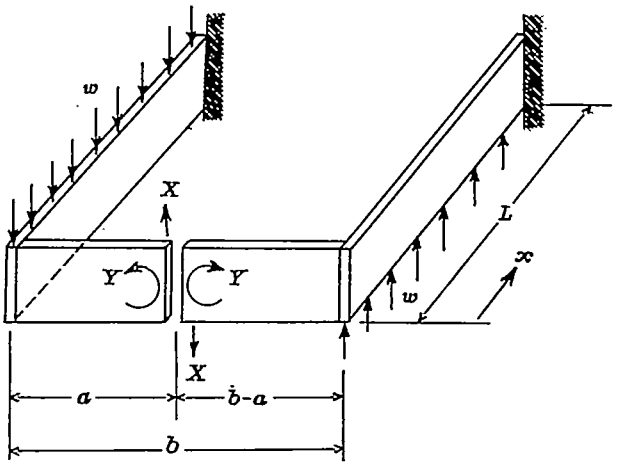

FIGURE 5.—Diagram for analysis of wing frame with one rib.

spacing may be considered as fixed by other design considerations, it is evident that an increase of relief action can be achieved only by increasing the torsional stiffnesses B of the spars.

In order to gain a quantitative idea of the torsional stiffness required for a desired amount of interaction, formula (6) may be used to establish a relief coefficient, giving the ratio of the relief moment at the wing root to the external bending moment:

$$C_R=\frac{m}{M_e} \tag{7}$$

For uniform loading and constant-spar sections, this becomes

$$C_R=\frac{3}{4\left(1+3\frac{b^2A_0}{L^2B_0}\right)} \tag{7a}$$

Using an average value of $\frac{b}{L}=\frac{1}{5}$ and replacing A_0 by $\frac{1}{2}A_F$, B_0 by $2B_F$ (i.e., assuming front and rear

spars to be equal) reduces (7a) to

$$C_R=\frac{1}{\frac{4}{3}+\frac{1}{25}\frac{A_F}{B_F}} \tag{7b}$$

Assuming a reduction in bending moment of 5 percent as the minimum worth considering, and adding to this another 5 percent for inefficiency of joints and deflection of ribs, we obtain $C_R=0.10$ as the minimum requirement. Equation (7b) then gives a maximum permissible value of $A_F/B_F=217$. A comparison of the A/B values for the rectangular beam and the routed beam of appendix A shows that the rectangular beam is within this limit, but that the routed beam has insufficient torsional stiffness to justify calculations for transference action.

Formula (7a) shows that the relief action disappears if the torsional stiffness B approaches zero; if B approaches infinity, the relief coefficient approaches the value ¾, corresponding to a beam built in at one end and supported at the other.

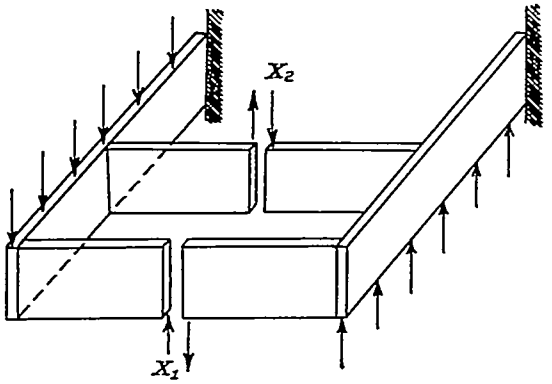

FIGURE 6.—Diagram for analysis of wing frame with two ribs.

Influence of location of rib along span.—The rib need not necessarily be located at the tip, but may be anywhere along the span. It is difficult to make any precise statements as to the best location for maximum effectiveness, since too many factors enter into the problem. In the first place, there is no simple criterion for effectiveness. The reduction in bending moment at the root was used in a preceding paragraph, but the reduction in moment all along the span should be considered to obtain a complete picture. Furthermore, the force in the rib depends on the relative values of the bending and torsional stiffnesses of front and rear spars, and these are capable of so many variations that a detailed discussion appears useless.

Generally speaking, it may be said that the maximum effects are secured by having the rib close to the tip of the wing. The extreme tip is the best place for the rib if the spars have constant sections and have vanishing torsional stiffness. If the spars taper, or if they have a very high torsional stiffness, the best position for the rib is farther inboard. For normal amounts of taper and torsional stiffness, the best location is usually in the outer third of the semispan.

Two practical considerations are in favor of placing the rib farther out than the best position for theoretical maximum relief moment in the spar. The farther inboard the rib is located the higher the force in it, unless the torsional stiffness is very low, so that the rib must be made very heavy to secure the necessary stiffness and strength. Furthermore, the relative motion of the two spars becomes rapidly less as the wing root is approached; consequently, the importance of the unavoidable play in the fittings increases rapidly and may vitiate any conclusions drawn on the basis of calculations assuming perfect joints. If desired, the effects of imperfect joints and of deformation of the rib may be taken into account when making the calculations but it is obvious that no general rules for locating the rib can be made, since allowances for such deviations from the fundamental assumptions depend entirely on the type of design.

WING FRAMES WITH MORE THAN ONE RIB

Standard methods of analysis.—The application of a conventional method of analysis will be briefly sketched for the case of a frame with two ribs (fig. 6). The first step is to calculate the locations of the cuts in the ribs by equation (3). If they do not fall in the same chordwise location, the distances may be averaged, giving the points closer to the spanwise center line of the frame more weight. An approximation that is always conservative for the spars is to make the cuts at the center line of the frame. The error committed by so doing is appreciable only if the spars have very low torsional stiffness, and if there is a large difference between the bending stiffnesses of the front and the rear spar. For $\frac{b}{L}=\frac{1}{5}$ and $I_R=\frac{1}{3}I_F$, the error in X is 11 percent for the box spar of appendix A and 21 percent for the rectangular spar.

Cutting the ribs introduces one unknown for each rib and one condition: The relative vertical displacement at each cut due to the external loads must equal the vertical displacement due to the unknowns X_1 and X_2 or

$$y_{1_e}=y_{1,1}X_1+y_{1,2}X_2 \tag{8a}$$

$$y_{2_e}=y_{2,1}X_1+y_{2,2}X_2 \tag{8b}$$

where $y_{1,2}$ is the deflection at cut 1, due to a unit force acting at 2. As in the case of the single rib, all coefficients connected with the unknowns contain two terms, one due to bending and one due to torsion. The coefficients can be computed for any given numerical case and substituted in the equations (8a) and (8b). The solution of these two simultaneous equations offers no difficulties.

For designers who prefer least-work methods, Mr. C. P. Burgess of the Bureau of Aeronautics, Navy Department, has proposed the following method of solution:

Consider as statically determinate structures the two spars, endowed with bending stiffness only, and as redundancies the torsional stiffnesses B_0 in each bay. Denote by R_n the fraction of the total torque in bay n taken up by torsional stresses; by M_s the bending moments in the spars with the ribs cut; by M_n the bending moments in the spars due to a pair of torque moments, equal in magnitude to the width of the bay, applied through the drag bracing at the outboard and the inboard end of bay n; and by l the length of the bay.

The following system of equations may now be written:

$$R_1\sum\left[\int\frac{M_1^2}{A}dx+\frac{T_1^2l}{B}\right]+R_2\sum\int\frac{M_1M_2}{A}dx+\sum\int\frac{M_sM_1}{A}dx=0 \tag{9a}$$

$$R_1\sum\int\frac{M_1M_2}{A}dx+R_2\sum\left[\int\frac{M_2^2}{A}dx+\frac{T_2^2l}{B}\right]+\sum\int\frac{M_sM_2}{A}dx=0 \tag{9b}$$

When these equations have been solved for R_1 and R_2 the final bending moments are obtained from

$$M=M_s+R_1M_1+R_2M_2 \tag{9c}$$

The physical concept behind this method is the same as for the first method outlined; the labor of computation is considerably lessened, however, through the introduction of equal and opposite couples at the end of each bay in place of the single couples Xb used in the first method.

If there are more than three or four ribs, the procedure becomes very laborious both in the computation of the coefficients and the solution of the system of equations. Thalau (reference 5) has nevertheless made several series of such calculations and, although the results are only of general interest on account of the assumptions made (constant and equal-spar sections), some interesting conclusions can be drawn from these calculations. The most important conclusion is that the tip rib gives practically all of the relieving effect, and that additional ribs in the span have little effect, no matter how many ribs are added or where they are located. Concordant with this fact, the forces in these additional ribs are usually smaller than the force in the tip rib, except for spars with unusually large torsional stiffnesses.

If the cross sections of the spars vary along the span, the situation is similar to that of a wing frame with a single rib. In general, the most advantageous locations for two ribs would be at the tip and at approximately two-thirds of the semispan from the root.

In view of the results of Thalau's calculations on spars with constant sections, it seems safe to assume that good approximations for the bending moments in the spars and the force in the tip rib will be obtained for any case of more than two ribs by assuming that only the tip rib and a rib at two-thirds of the span are operative. This statement will be corroborated later on by comparison with other methods of calculation.

The approximate method of calculation has the drawback of not giving the forces in the intermediate ribs. It has already been pointed out, however, that for the inboard portion of the wing, calculations may be largely illusory due to deformations and the effects of play in fittings; consequently, judicious estimates based on the force in the tip rib are probably of as much practical value as more exact calculations.

It may be mentioned that attempts have been made to solve the problem of the multirib wing frame from the opposite point of view, i.e., by assuming that there are infinitely many ribs and setting up the differential equations for two spars connected by a continuous elastic coupling. Reference 6 gives such a solution and a very complete discussion of the fundamental case of constant sections with uniform load. For variable sections and loads, successive approximation methods have been proposed (see bibliography in reference 6) for integrating the differential equations, but they are in too mathematical a form to appeal to the stress-analyst. As a matter of some interest, the formulas for the angle of twist at the tip of a wing with constant-section spars will be given here.

(a) For a torsional moment T consisting of two equal and opposite forces applied at the tip

$$\theta=\frac{TL}{B_0}\left(1-\frac{\tanh\ \lambda L}{\lambda L}\right) \tag{10a}$$

(b) For a torsional moment produced by equal and opposite uniform running loads w along the spars

$$\theta=\frac{wA_0b^3}{B_0^2}\left(1+\frac{1}{2}\lambda^2L^2-\lambda L\tanh\lambda L-\operatorname{sech}\lambda L\right) \tag{10b}$$

where

$$\lambda^2=\frac{B_0}{A_0b^2}$$

The Friedrichs-von Kármán equations.—The conventional methods of analysis become very cumbersome for practical use for more than three or four unknowns if no sweeping simplifying assumptions are made. Two main defects of these methods are apparent: When the coefficients are calculated, it is necessary to consider the properties of a large part of the wing frame and to make lengthy numerical integrations; furthermore, unless certain combinations of the forces X_1, X_2, etc., are used as unknowns, the resulting system of equations involves each unknown in each equation, thus producing a system which is difficult to solve by ordinary means.

Friedrichs and von Kármán have shown a solution of the difficulty (reference 2). They point out that each spar may be considered as a continuous beam over a number of elastically yielding supports, the ribs, which in turn derive their load-bearing ability from the other spar. Convenient methods for dealing with continuous beams are well known, one of them being the method of "3-moment equations"; the Friedrichs-von Kármán equations are essentially a set of 3-moment equations applied to a wing frame. The derivation of these equations will now be given.

Figure 7 shows part of a wing frame consisting of two parallel spars connected by a number of ribs. The ribs are numbered, beginning with zero at the wing tip, and each bay carries the same number as the rib at its inboard end. In order to investigate the internal forces in the spars, the spars have been cut just out-

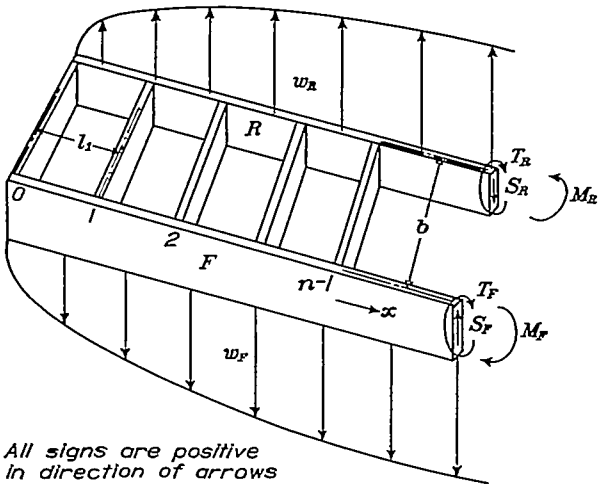

FIGURE 7.—Free-body diagram of wing frame with many ribs.

board of the nth rib. The forces acting on the face of each cut are a shearing force S, a bending moment M, and a torsional moment T. The external load consists of a running load w on each spar, which need not be uniform along the span, but is subjected only to the condition that at any point $w_F=w_R$. The opposite sense of forces and bending moments in the two spars is taken care of by the sign convention adopted. Since $w_F=w_R$, the external shears and bending moments (without interaction) at any point are also equal in the front and rear spars, so that no subscripts denoting front or rear are needed, but only subscripts denoting the spanwise location, and we may write

$$\int_{\cdot}^{n} w\,dx=S_{e_n}=\left(\frac{dM_e}{dx}\right)_n \qquad (FK\text{–}1)$$

Of the three significant equations of static equilibrium, two state that the internal shears and bending moments are also equal in the front and rear spars

$$S_F=S_R=S,\ M_F=M_R=M \qquad (FK\text{–}2)$$

The third equation of equilibrium gives

$$T_F+T_R+b(S-S_e)=0 \qquad (FK\text{–}3)$$

Now, remembering that $S=\frac{dM}{dx}$ and defining the relief moment m by

$$M=M_e+m \qquad (FK\text{–}4)$$

equation (FK—3) may be transformed to

$$T_F+T_R+b\frac{dm}{dx}=0 \qquad (FK\text{–}5)$$

(From $M_{e_F}=M_{e_R}$ and $M_F=M_R$ it follows that $m_F=m_R$.)

The relief moments m_F and m_R are due to the concentrated forces exerted on the spars by the ribs; therefore, they are linearly distributed between stations, and

$$\left(\frac{dm}{dx}\right)_n=\frac{m_n-m_{n-1}}{l_n}$$

which may be substituted into the last equation to give

$$T_F+T_R+b\frac{m_n-m_{n-1}}{l_n}=0 \qquad (FK\text{–}6)$$

The torque (T_F+T_R) remains constant for the length of one bay. Since the spars are assumed to be rigidly connected at each station by the rib, and consequently the twist of the front spar between stations $n-1$ and n must equal the twist of the rear spar between these stations, the relation between the torques T_F and T_R is given by

$$\frac{T_F}{T_R}=\frac{B_F}{B_R} \qquad (FK\text{–}7)$$

where B is again the torsional stiffness of the spar section. If B varies between stations, the average defined by

$$\frac{1}{B_n}=\frac{1}{l_n}\int_{n-1}^{n}\frac{dx}{B_x} \qquad (FK\text{–}8)$$

must be used.

Equations (FK–6) and (FK–7) combine to give

$$\begin{aligned} T_{F_n}&=-(m_n-m_{n-1})\frac{b}{l_n}\left(\frac{B_F}{B_F+B_R}\right)_n \\ T_{R_n}&=-(m_n-m_{n-1})\frac{b}{l_n}\left(\frac{B_R}{B_F+B_R}\right)_n \end{aligned} \qquad (FK\text{–}9)$$

Since all static equations have been satisfied, the principle of least work can now be applied to find

the relief moments. The internal work done in the structure is

$$W=\frac{1}{2}\sum\int\frac{M^2\mathrm{d}x}{A_F}+\frac{1}{2}\sum\int\frac{M^2\mathrm{d}x}{A_R}+\frac{1}{2}\sum\int\frac{T_F{}^2\mathrm{d}x}{B_F}+\frac{1}{2}\sum\int\frac{T_R{}^2\mathrm{d}x}{B_R} \tag{FK–10}$$

In this expression, each integral extends over one bay, while the summation signs extend over the whole wing. Using equations (FK–4) and (FK–9), M and T can be expressed in terms of known quantities and of the relief moments. When these substitutions have been made in equation (FK–10), the partial derivative of the work can be taken with respect to m_1, m_2, m_3 . . . m_n, furnishing one equation for each unknown relief moment by equating each derivative to zero.

On account of the linear distribution of m between bays, the general expression for m at any point within bay n is

$$m_x=m_{n-1}\frac{l_n-x}{l_n}+m_n\frac{x}{l_n} \tag{FK–11}$$

where for convenience the origin of the x axis is taken at the lower-numbered end of the bay under consideration.

It will be seen that when the derivative is taken with respect to any moment m_n, the summation will extend over only two bays: Bay n from station n–1 to n and bay n+1 from station n to n+1. The result is

$$\frac{\partial W}{\partial m_n}=\int_{n-1}^{n}\frac{M_e}{A_0}\frac{x}{l}\mathrm{d}x+\int_{n-1}^{n}\frac{1}{A_0}\left(m_{n-1}\frac{l-x}{l}+m_n\frac{x}{l}\right)\frac{x}{l}\mathrm{d}x+\int_{n}^{n+1}\frac{M_e}{A_0}\frac{(l-x)}{l}\mathrm{d}x+\int_{n}^{n+1}\frac{1}{A_0}\left(m_n\frac{l-x}{l}+m_{n+1}\frac{x}{l}\right)\frac{l-x}{l}\,\mathrm{d}x+\left(\frac{b^2}{lB_0}\right)_n(m_n-m_{n-1})-\left(\frac{b^2}{lB_0}\right)_{n+1}(m_{n+1}-m_n)=0 \tag{FK–12}$$

where A_0 is defined as previously by $\frac{1}{A_0}=\frac{1}{A_F}+\frac{1}{A_R}$ and $B_0=B_F+B_R$. In each term, l is the length of the bay over which the integral extends.

Introducing the following abbreviations

$$\left.\begin{aligned}p_n&=\int_{n-1}^{n}\frac{M_e}{A_0}\frac{x}{l}\mathrm{d}x\\ q_n&=\int_{n-1}^{n}\frac{M_e}{A_0}\frac{(l-x)}{l}\,\mathrm{d}x\\ r_n&=\int_{n-1}^{n}\frac{x^2\mathrm{d}x}{l^2A_0}+\left(\frac{b^2}{lB_0}\right)_n\\ s_n&=\int_{n-1}^{n}\frac{x(l-x)\mathrm{d}x}{l^2A_0}-\left(\frac{b^2}{lB_0}\right)_n\\ t_n&=\int_{n-1}^{n}\frac{(l-x)^2\mathrm{d}x}{l^2A_0}+\left(\frac{b^2}{lB_0}\right)_n\end{aligned}\right\} \tag{FK–13}$$

the final system of equations reads

$$\left.\begin{aligned}m_1(r_1+t_1)+m_2s_2&=-(p_1+q_1)\\ m_1s_2+m_2(r_2+t_2)+m_3s_3&=-(p_2+q_2)\\ m_2s_3+m_3(r_3+t_4)+m_4s_4&=-(p_3+q_4)\\ &\cdots\\ &\cdots\\ m_{n-1}s_n+m_nr_n&=-p_n\end{aligned}\right\} \tag{FK–14}$$

The computation of the coefficients p, q, r, s, and t can be simplified by various assumptions. Whether or not these assumptions are admissible in any given case must be left to the judgment of the designer.

If five or more ribs are considered to be acting, it will be sufficiently accurate, in general, to use the values of A and B for the middle of each bay as the average values and to assume that the sections are constant for the length of one bay. With this assumption

$$\left.\begin{aligned}r_n&=\left(\frac{l}{3A_0}\right)_n+\left(\frac{b^2}{lB_0}\right)_n\\ s_n&=\left(\frac{l}{6A_0}\right)_n-\left(\frac{b^2}{lB_0}\right)_n\\ t_n&=r_n\end{aligned}\right. \tag{FK–15}$$

Assuming constant A and a linear variation of M for each bay gives

$$\left.\begin{aligned}p_n&=\left(\frac{l}{6A_0}\right)_n(M_{e_{n-1}}+2M_{e_n})\\ q_n&=\left(\frac{l}{6A_0}\right)_n(2M_{e_{n-1}}+M_{e_n})\end{aligned}\right. \tag{FK–16}$$

A somewhat better approximation for p and q is possibly obtained by assuming that M/A varies linearly (it is often practically constant), which gives

$$\left.\begin{aligned}p_n&=\frac{1}{6}l\left(\frac{M_{e_{n-1}}}{A_{0_{n-1}}}+\frac{2M_{e_n}}{A_{0_n}}\right)\\ q_n&=\frac{1}{6}\left(\frac{2M_{e_{n-1}}}{A_{0_{n-1}}}+\frac{M_{e_n}}{A_{0_n}}\right)\end{aligned}\right. \tag{FK–17}$$

If the assumption of constant A_0 in each bay does not appear to be sufficiently accurate, and linear variation from $A_{0_{n-1}}$ to A_{0_n} is assumed, the terms in r, s, t become, dropping the subscript zero

$$\left.\begin{aligned}r_n&=\frac{l}{(A_n-A_{n-1})^3}\left[\frac{1}{2}A_n{}^2-2A_nA_{n-1}+\frac{3}{2}A_{n-1}{}^2+A_{n-1}{}^2\log_e\frac{A_n}{A_{n-1}}\right]+\left(\frac{b^2}{lB_0}\right)_n\\ s_n&=\frac{l}{(A_n-A_{n-1})^3}\left[\frac{1}{2}A_n{}^2-\frac{1}{2}A_{n-1}{}^2\right.\end{aligned}\right. \tag{FK–18}$$

$$-A_nA_{n-1}\log_e\frac{A_n}{A_{n-1}}\Big]-\left(\frac{b^2}{lB_0}\right)_n$$

$$t_n=\frac{l}{(A_n-A_{n-1})^3}\Big[-\frac{3}{2}A_n^2+2A_nA_{n-1}-\frac{1}{2}A_{n-1}^2$$

$$+A_n^2\log_e\frac{A_n}{A_{n-1}}\Big]+\left(\frac{b^2}{lB_0}\right)_n$$

Attention should perhaps be called to the fact that the sign convention adopted for the front spar is opposite to the standard.

The general case of arbitrary loadings.—The separation of the load into a bending load and a torque load usually results in a reduction of the numerical work required, because the calculation of the interaction effect is made only once for the case of pure torque. Various flight conditions can then be investigated simply by superposing the effects of bending and torque loads in the proper proportions.

The direct analysis of any case of arbitrary loadings on front and rear spars, for example, the low angle-of-attack condition, may be made by any of the methods discussed. It is obvious that such a procedure of

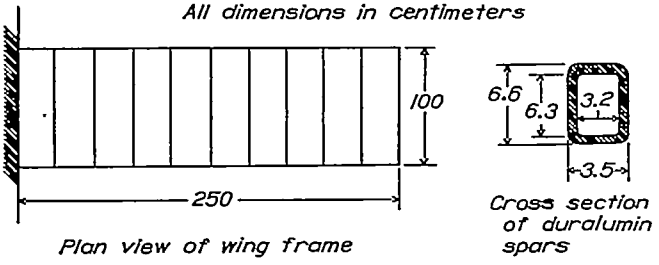

FIGURE 8.—Details of duralumin wing frame.

investigating each flight condition separately would be lengthy because each time the calculation of the interaction effect would be included. This method, however, does not require the knowledge of the elastic axis; it may therefore be preferable in cases where there is some doubt about the accuracy with which the elastic axis may be found.

The method of procedure to be used in the general case requires no comments if standard methods are used. If the Friedrichs-von Kármán equations are used, the following substitutions must be made in (FK–13):

$$p_n=\int_{n-1}^{n}\frac{M_{Fe}}{A_F}\frac{x}{l}dx+\int_{n-1}^{n}\frac{M_{Re}}{A_R}\frac{x}{l}dx$$

$$q_n=\int_{n-1}^{n}\frac{M_{eF}}{A_F}\left(\frac{l-x}{l}\right)dx+\int_{n-1}^{n}\frac{M_{eR}}{A_R}\left(\frac{l-x}{l}\right)dx \qquad \text{(FK–19)}$$

provided that the sign convention of figure 7 is retained. If the usual sign convention is adopted (up loads positive for both spars), the sign of the front spar term in p and q must be reversed.

NUMERICAL EXAMPLE FOR USE OF FORMULAS, WITH COMPARISONS BETWEEN THEORY AND EXPERIMENT

In order to show the application of the formulas developed, a metal wing frame will be calculated in detail. The dimensions of the frame and the test results are taken from reference 7. Figure 8 shows the dimensions of the wing frame and of the spar section (front and rear spars are identical). Since the absolute dimensions of the wing are such that it cannot be considered as a practical case, the metric units have not been converted into English units.

The properties of spars are computed as follows:

$I=17.1$ cm^4

$A_F=EI_F=EI_R=11.2\times10^6$ kg cm^2 (from bending test on spar)

$$\frac{1}{A_0}=\left(\frac{1}{11.2}+\frac{1}{11.2}\right)\times10^{-6}$$

$A_0=5.6\times10^6$ kg cm^2

$J_F=$(formula (T–3), appendix A)$=14.3$ cm^4

$G=285{,}000$ kg cm^2 (from tests on round tubes)

$B_F=GJ_F=GJ_R=4.07\times10^6$ kg cm^2

$B_0=(4.07+4.07)\times10^6=8.14\times10^6$ kg cm^2

The loading condition chosen here for comparison with test results is a 40-kilogram load applied at the tip of the front spar. Since the two spars are alike, the elastic axis of the wing frame is at the center line, and the load may be resolved into a bending load of 40 kilograms at the center line and a torque of $40\times50=2{,}000$ cm-kg. The vertical deflection at the tip due to the bending load is

$$y_1=\frac{20\times250^3}{3\times11.2\times10^6}=9.30\text{ cm}$$

independent of the numbers of ribs acting. The deflections due to the torque will be computed for two cases: all ribs acting, and tip rib only acting.

Since the case of 10 ribs acting is practically a close approach to an infinite number of ribs acting, formula (10a) may be used here. The parameter λ is found from

$$\lambda^2=\frac{B_0}{A_0b^2}=\frac{8.14\times10^6}{5.6\times10^6\times100^2}=1.453\times10^{-4}$$

$\lambda=1.206\times10^{-2}$; $\lambda L=3.015$; $\tanh\ \lambda L=0.995$

$$\theta=\frac{2{,}000\times250}{8.14\times10^6}\left(1-\frac{0.995}{3.015}\right)=0.0411$$

$$y_2=\theta\times\frac{b}{2}=2.05\text{ cm}$$

For the case of the tip rib only acting, a formula similar to formula (6) can be derived

$$X=\frac{P}{1+3\frac{b^2}{L^2}\frac{A_0}{B_0}}$$

where P is defined by $P=T/b=20$ kg

Substituting the numerical values gives

$$X=0.752\ P=15.04\text{ kg}$$

Consequently, the tip deflection due to torque is for this case

$$y_3=\frac{4.96\times250^3}{3\times11.2\times10^6}=2.31 \text{ cm}$$

The total deflections of the front-spar tip are therefore

$y=y_1+y_2=11.35$ cm for all ribs acting

$y=y_1+y_3=11.61$ cm for tip rib only acting

The experimental values are 11.13 and 11.33 respectively.

In order to simplify the calculation of the moments by means of the Friedrichs-von Kármán formulas, it will be assumed that only five ribs are working.

$$l_1=l_2=l_3=l_4=l_5=50 \text{ cm}$$

Using equation (FK–15):

$$r_1=r_2=r_3=r_4=r_5=t_1=t_2=t_3=t_4=t_5$$
$$=\frac{50}{3\times5.6\times10^6}+\frac{100^2}{50\times8.14\times10^6}$$
$$=(3.0+24.6)\times10^{-6}=27.6\times10^{-6}$$
$$s_1=s_2=s_3=s_4=s_5=(1.5-24.6)\times10^{-6}=-23.1\times10^{-6}$$

For this calculation let $P=1$, on each spar tip (T=100), which gives

$$M_{e_0}=0 \quad M_{e_1}=50 \quad M_{e_2}=100$$
$$M_{e_3}=150 \quad M_{e_4}=200 \quad M_{e_5}=250 \text{ cm-kg}$$

Using equation (FK–16):

$$p_1=\frac{50}{6\times5.6\times10^6}(0+2\times50)=149.0\times10^{-6}$$
$$p_2=\frac{50}{6\times5.6\times10^6}(50+2\times100)=372.5\times10^{-6}$$
$$p_3=\frac{50}{6\times5.6\times10^6}(100+2\times150)=596.0\times10^{-6}$$
$$p_4=\frac{50}{6\times5.6\times10^6}(150+2\times200)=819.5\times10^{-6}$$
$$p_5=\frac{50}{6\times5.6\times10^6}(200+2\times250)=1{,}043.0\times10^{-6}$$
$$q_1=1.490\times10^{-6}(0+50)=74.5\times10^{-6}$$
$$q_2=1.490\times10^{-6}(2\times50+100)=298\times10^{-6}$$
$$q_3=1.490\times10^{-6}(2\times100+150)=521.5\times10^{-6}$$
$$q_4=1.490\times10^{-6}(2\times150+200)=745\times10^{-6}$$
$$q_5=1.490\times10^{-6}(2\times200+250)=968.5\times10^{-6}$$

With these values of p, q, r, s, and t the following system of equations is obtained

$$m_1\times55.2-m_2\times23.1=-447$$
$$-m_1\times23.1+m_2\times55.2-m_3\times23.1=-894$$
$$-m_2\times23.1+m_3\times55.2-m_4\times23.1=-1{,}341$$
$$-m_3\times23.1+m_4\times55.2-m_5\times23.1=-1{,}788$$
$$-m_4\times23.1+m_5\times27.6=-1{,}043$$

These equations may be solved by expressing m_4 as a function of m_5 in the last equation, then successively expressing m_3, m_2, and m_1 as functions of m_5; two equations for m_1 will be obtained which can be used to calculate m_5. Substitution of m_5 in the previously obtained expressions will then give m_1, m_2, m_3, and m_4.

In certain cases, the method of solution indicated will give the result as the difference of numbers too large to be handled even on a calculating machine. In such cases the solution can be effected by a process of successive approximations. Assume reasonable values for the relief moments m along the span and, starting with the last equation, solve each equation in turn for the unknown with the largest coefficient. Repeat the process with the corrected values for the unknowns until two successive values are in sufficiently close agreement. This method of solving the system of equations is very rapid if the coefficients (r_n+t_{n+1}) are 5 to 10 times larger than the coefficient s_n, a condition applying particularly to stressed-skin wings.

Table I gives the results of the calculations for the present example in the following sequence:

(1) The external bending moment (for a tip load of $P=1$) on each spar.

(2) The relief moments m_1 to m_5.

(3) The resulting bending moments (sum of (1) and (2) by equation (FK–4)), equal and opposite for front and rear spar.

(4) The differences between successive values of m.

(5) The total torque carried by torsional shear of the spars in each bay (equation (FK–6))

$$T_1=T_F+T_R=\frac{b}{l_n}(m_n-m_{n-1})$$

(6) The bending shear in the spars for each section, $S=\frac{dM}{dx}$; in this case, since the moment distribution along the span is linear, between stations $S=\frac{M_n-M_{n-1}}{l_n}$.

(7) The torque carried in each bay by the bending shear in the spars $T_2=Sb$.

As a check, it will be noted that $T_1+T_2=T_s$.

TABLE I.—INTERNAL FORCES AND MOMENTS IN WING FRAME OF REFERENCE 7

[Loading: 1 kg down at tip of front spar, 1 kg up at tip of rear spar]

Station	M_e, cm-kg	m, cm-kg	M, cm-kg	m_n-m_{n-1}	T_1, cm-kg	S, kg	T_2, cm-kg
0	0	0	0				
				44.3	88.6	0.114	11.4
1	50	−44.3	5.7				
				43.4	86.8	.132	13.2
2	100	−87.7	12.3				
				38.0	76.0	.240	24.0
3	150	−125.7	24.3				
				29.5	59.0	.410	41.0
4	200	−155.2	44.8				
				12.5	25.0	.760	75.0
5	250	−167.7	82.3				

The results are plotted in figure 9. The figure shows the external bending moments M_e, the bending moments M with the tip rib acting, the bending

moments M with five ribs acting, and the variation of T_1 and T_2 along the span. It is apparent that near the tip the largest part of the external torque is carried by the torsional stresses in the spars but that, as the root is approached, the part of the torque carried by bending of the spars rapidly increases and is the major part near the root.

The values of M given in table I may be used to calculate the bending deflection at the tip due to the torque, it being remembered that the actual torque is exerted by $P=\pm 20$ kg on the spar tips. Numerical integration of these values gave $y=2.03$ cm, as compared with $y=2.05$ cm obtained from formula (8) and $y=2.31$ cm obtained by assuming that only the tip rib is acting. It will be seen that the percentage difference in tip deflection is very much less than the

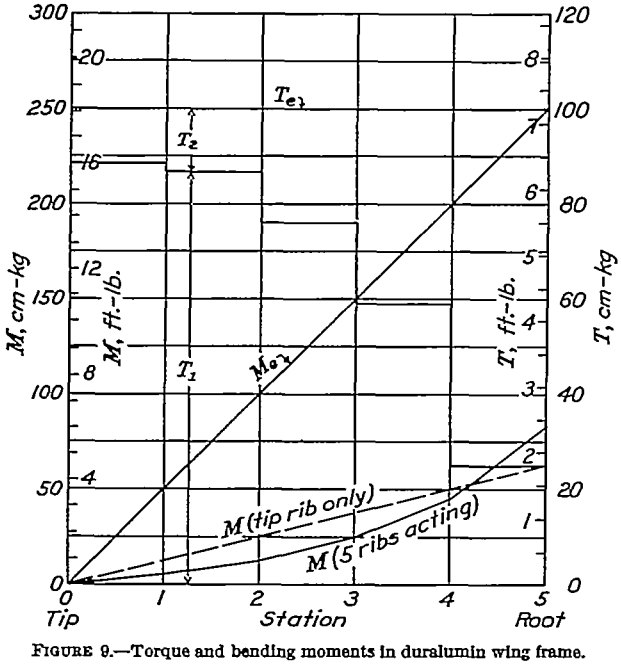

FIGURE 9.—Torque and bending moments in duralumin wing frame.

differences in bending moments along the span for the two cases of tip rib acting and all ribs acting, the latter differences being more than 100 percent in places, as shown in figure 9. This fact means that ordinary deflection measurements are of little value for tests of this nature; in order to obtain the accuracy required, it will be necessary either to measure the slope of the elastic line or to make strain measurements.

A number of strain measurements was made on the frame under consideration (reference 7), and figure 10 shows the results for the loading case computed in the preceding example. The figure gives the bending moments due to the direct bending load of 40 kilograms applied at the elastic center of the wing, the total computed moment (using the values of M of table I), and the bending moments computed from the strain measurements. The agreement is good, the only possible objection to the test procedure being that equal and opposite loads should have been applied to both spars so as to eliminate the direct bending load and thus considerably increase the accuracy of checking the amount of relief action, which influences only the part between the two curves of bending moments.

A wing frame consisting of two wooden box spars connected by 10 ribs was tested by von Fákla (reference 8). As a result of this test and a test on a full-sized metal wing, von Fákla concluded that the interaction can be calculated to an accuracy of better than 5 percent. This conclusion, of course, involves the presumption that the properties of the spars are known with the same accuracy, a presumption hardly warranted in any given case for wood construction, since the material properties E and G are variable in much wider limits.

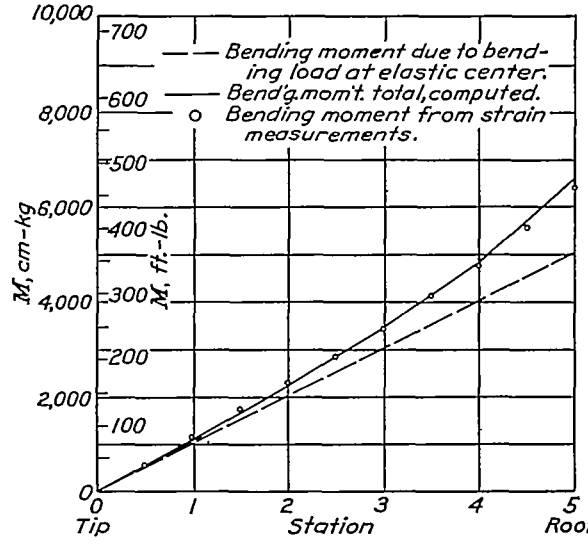

FIGURE 10.—Computed and measured bending moments in duralumin wing frame.

WING FRAMES WITH DRAG BRACING IN TWO PLANES AND PARALLEL SPARS

PRINCIPLE OF CALCULATION

The Friedrichs-von Kármán formulas were derived for a wing frame in which the drag bracing is arranged in a single plane, so that pure torsional stiffness (i.e., torsional stiffness outside of that obtained by bending of the spars) is furnished only by the individual torsional stiffnesses of the spars. However, it is quite well appreciated that double drag bracing, be it wire or stressed skin, furnishes a much higher torsional stiffness than can normally be obtained from the spars alone, provided that the two planes of drag bracing are well separated.

From the derivation of the Friedrichs-von Kármán formulas, it is clear that they still hold if the pure torsional stiffness of a wing section is furnished by other means than by having spars possessing individual torsional stiffness. The necessary torsional stiffness may be achieved by connecting the spars in the top and bottom planes by drag-wire bracing, thus closing the space between the spars to form a torsion box; or

the wing may be covered with a stressed skin, converting the whole wing section into a torsionally stiff shell. The wing must then be considered to consist of two distinct elements: One element stressed in bending, the spars; and one element stressed in torsion, the torsion tube. The spar webs thus may perform a dual function: They may at the same time be part of the bending element and also part of the torsion tube. The shearing stress in the webs is obtained by superposing the shear due to torsion of the torsion tube (uniformly distributed over the depth of the web) and the shear due to bending of the spars (parabolically distributed over the depth unless diagonal-tension fields form).

The pure torsional stiffness of torsion tubes is calculated by formula (T–3), appendix A. In the case of drag-wire bracing, it is expedient to calculate an effective skin thickness of an imaginary skin such that the shear deformation of this skin is equal to the shear deformation of a panel due to the elongation of the wires.

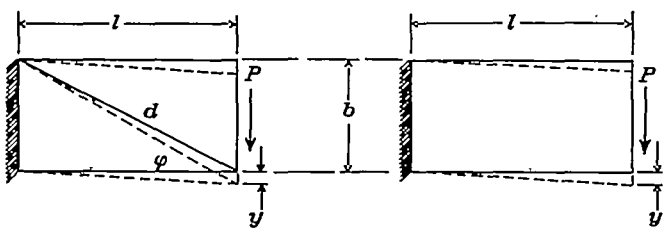

FIGURE 11.– Shear deflection of truss panel and solid sheet.

For the wire-braced panel we have (fig. 11)

$$y=P\frac{d^3}{b^2AE}$$

where A is the cross-sectional area of the diagonal.

For the solid sheet

$$y=P\frac{l}{bt_eG}$$

Equating the deflection and solving for the equivalent thickness

$$t_e=\frac{lbAE}{d^3G}=\frac{EA}{G\,l}\sin\varphi\cos^2\varphi \qquad (11)$$

For the panel of figure 12, consisting of steel spars with steel-wire bracing, the torsional stiffness becomes (assuming E the same for tubes and wires)

$$GJ=\frac{4A^2G}{\int\frac{ds}{t}}=\frac{4h^2b^2G}{\frac{2b}{t_1}+\frac{2h}{t_2}}$$

Now

$$t_1=\frac{E}{G}\frac{A_D}{l}\sin\varphi_1\cos^2\varphi_1$$

$$t_2=\frac{E}{G}\frac{A_d}{l'}\sin\varphi_2\cos^2\varphi_2$$

$$b=l\tan\varphi_1;\quad h=l'\tan\varphi_2$$

Therefore, by substitution

$$GJ=\frac{2h^2b^2E}{\left[\frac{l^2}{A_D\cos^3\varphi_1}+\frac{l'^2}{A_d\cos^3\varphi_2}\right]} \qquad (12)$$

The computation of t_2 need not be very exact, as a rule, since t_1 is the decisive factor, the area of the tubes in the spar web being much larger than that of the wires. Average values may be used for φ_2 and A_d if these values change in the bay.

A word of caution appears very necessary regarding the value of G to be used for stressed-skin wings, particularly plywood-covered wings. The shearing modulus has not been used very extensively in engineering in the past; the results of only a few tests on different materials are scattered through the literature, and they have often been obtained by very questionable methods. Only results obtained from torsion tests should be used, if obtainable. Appendix B

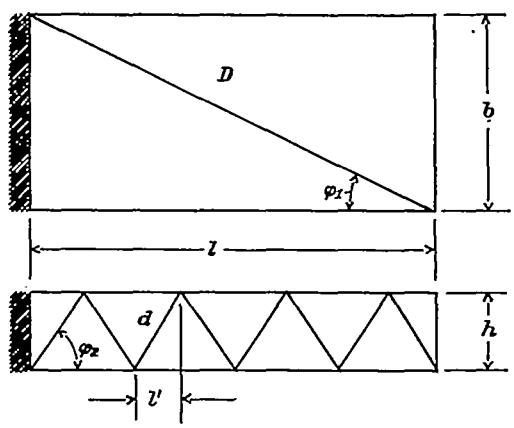

FIGURE 12.—Diagram of trussed wing panel.

gives a collection of such data as were available to the writer.

Attention must be called to the fact that the wing covering may buckle at very low loads to form diagonal-tension fields. When a sheet of thickness t has buckled, it has a reduced effective thickness of

$$t_e=\frac{tE}{4G} \qquad (13)$$

or for duralumin and steel, $t_e=\frac{5}{8}t$. This relationship is based on the elementary theory of diagonal-tension fields, and it involves the assumption that the flanges are infinitely rigid and that the tension folds are inclined at 45° against the beam axis. Formulas for calculating the buckling stress may be found in good textbooks on strength of materials. In calculations of this nature, the edges should be assumed to be simply supported, because the elastic restraint that actually exists is canceled by the detrimental effect of initial buckles.

NUMERICAL EXAMPLE OF WING FRAME WITH DOUBLE DRAG-WIRE BRACING, INCLUDING COMPARISON BETWEEN THEORY AND EXPERIMENT

A very suitable example of this type of structure is a wing frame that was built for testing purposes at Wright Field. The dimensions of this frame, test results, and results of least-work calculations treating the whole frame as a pin-jointed space structure are given in reference 9. For convenience, the dimensions are given in figure 13 of the present report and the results of one set of least-work calculations are given in figure 14, which is taken from figure 30 of reference 9.

TABLE II.—INTERNAL FORCES AND MOMENTS IN WING FRAME OF REFERENCE 9

[Loading: 100 pounds down at tip of the front spar; 100 pounds up at tip of the rear spar]

Station	1	2	3	4	5	6	7	8	9	10	11	12	13	14	15	16
											Front spar			Rear spar		
	M_s, in.-lb.	m, in.-lb.	M, in.-lb.	Δm, in.-lb.	T_1, in.-lb.	f_s, lb./in.	S (drag truss), lb.	F (drag wire), lb.	ΔM, in.-lb.	S (spar web), lb.	S (torsion), lb.	S (total), lb.	F (web diag)., lb.	S (torsion), lb.	S (total), lb.	F (web diag.), lb.
0	0	0	0													
				2,912	2,425	5.38	161.4	252	688	19.1	48.4	67.5	95.5	32.3	51.4	92.5
1	3,600	−2,912	688													
				2,656	2,210	4.91	147.3	230	944	26.2	44.2	70.4	99.5	29.5	55.7	100.4
2	7,200	−5,568	1,632													
				2,051	1,710	3.80	114.0	177.9	1,549	43.0	34.2	77.2	109.1	22.8	65.8	118.7
3	10,800	−7,619	3,181													
				871	726	1.613	48.4	75.5	2,729	75.8	14.5	90.3	127.8	9.7	85.5	164.1
4	14,400	−8,490	5,910													

The bending and torsional stiffnesses were calculated as follows:

Moments of Inertia

Front spar: $I=2\times0.1656\times4.5^2=6.70$ in.^{4}; $E=29\times10^6$; $EI=194.3\times10^6$ lb.in.^{2}

Rear spar: $I=2\times0.1656\times3^2=2.98$ in.^{4}; $EI=86.3\times10^6$ lb.in.^{2}

$$\frac{1}{A_0}=\frac{1}{194.3}+\frac{1}{86.3}\times10^6=0.01674\times10^{-6}\quad A_0=59.8\times10^6 \text{ lb.in.}^2$$

TORSIONAL STIFFNESS OF BOX SECTION

Equivalent thicknesses of solid sheet (formula (11))

$$\text{Drag truss:}\quad t_1=\frac{30\times10^6}{G}\times0.0141\times\frac{1}{36}\times0.641\times0.769^2=4{,}450\,\frac{1}{G}$$

$$\text{Front-spar web:}\quad t_2=\frac{29\times10^6}{G}\times0.0786\times\frac{1}{9}\times0.707\times0.707^2=89{,}500\,\frac{1}{G}$$

$$\text{Rear-spar web:}\quad t_3=\frac{29\times10^6}{G}\times0.0786\times\frac{1}{9}\times0.555\times0.832^2=97{,}300\,\frac{1}{G}$$

$$B=GJ=\frac{4A^2G}{\int\frac{ds}{t}}=\frac{4\times225^2}{\frac{60}{4{,}450}+\frac{9}{89{,}500}+\frac{6}{97{,}300}}=14.87\times10^6 \text{ lb.in.}^2$$

It will be noted that the shear deflections of the spars were neglected in computing the bending stiffness, resulting in overestimating the stiffnesses, consequently the loads calculated for the spars. In this particular case, however, the error is not much larger than the possible uncertainties; furthermore, the test loads are introduced as vertical loads at the spars, and the transference of the loads from the spars to the drag trusses is not perfect as assumed by theory, so that the approximate bending stiffnesses are sufficiently accurate for the purpose of calculating the interaction effect.

With the calculated values of A_0 and B_0 the relief moments are calculated in the same manner as for the duralumin wing frame (fig. 8). Column 1 of table II gives the external bending moment for a down load $P=100$ pounds on the front spar and an equal up load on the rear spar. Column 2 gives the calculated relief moments; column 3 gives the actual bending moment in the spars, obtained as the sum of columns 1 and 2. Column 4 gives the difference between relief moments at successive stations; this difference multiplied by b/l gives the torque T_1 carried by the torsion box, which is listed in column 5; column 6 gives the

shear force per inch of perimeter in the torsion box, obtained from $f_s t_c = \frac{T}{2A}$ where A=area of torsion tube. The total shearing force for one drag truss, column 7, is multiplied by 1.56 to give the force in the drag wire, column 8. Column 9 gives the increments in bending moments, which are used to compute the bending shears listed in column 10. Column 11 gives the torsional shear in the front spar, obtained by multiplying the shear force per inch perimeter (column 6) by the depth of the spar. Column 12 gives the total shear in the front spar, obtained by adding the values of columns 10 and 11. Finally, column 13 gives the forces in the diagonals of the spar web, calculated from the shears of column 12. Columns 14, 15, and 16 give the shear calculations for the rear spar.

The forces in the spar flanges are obtained by superposing the forces due to the bending moments and the forces due to the torsional shear. Take, as an example, the forces in the second bay from the tip of the front spar. Member e–d (fig. 13) transmits the full shear (i.e., compression due to the tension of the drag wire) to the amount of $f_s t_c l = 4.91 \times 36 = 177$ pounds. The force due to the bending moment is $\frac{1,632}{9} = 181$ pounds; therefore the force in member e–d is 358 pounds.

Passing from member e–d to member g–d, the shear force in the flange is reduced by the amount carried over into the web members at the joint between e–d and g–d; this reduction equals $4.91 \times 18 = 88$ pounds, leaving 89 pounds to be taken care of in the flange; the force due to bending in member g–d is $\frac{1,160}{9} = 129$ pounds, making the total force 218 pounds. Passing now to member i–d, all of the torsional shear has been transmitted to the web, so that the force in i–g is only that due to bending.

Figure 14 is a reproduction of the results of least-work calculations reported in reference 9. Unfortunately, the reference does not state whether the values used in these calculations for tube areas, wire areas, moduli of elasticity, etc., were actual or nominal. In the calculations made by the writer, nominal sizes and standard values were used; it will be seen that the results given in the preceding paragraph and in columns 8, 13, and 16 of table II agree with the values given in figure 14 within the limits of the accuracy of calculation.

The same wing frame was calculated with ¼–28 wire in place of the 10–32 wires. The agreement with the least-work calculations was not so good as in the previous case, but the differences were only about 5 percent when the maximum wire area permissible under the materials specifications was used in the calculation.

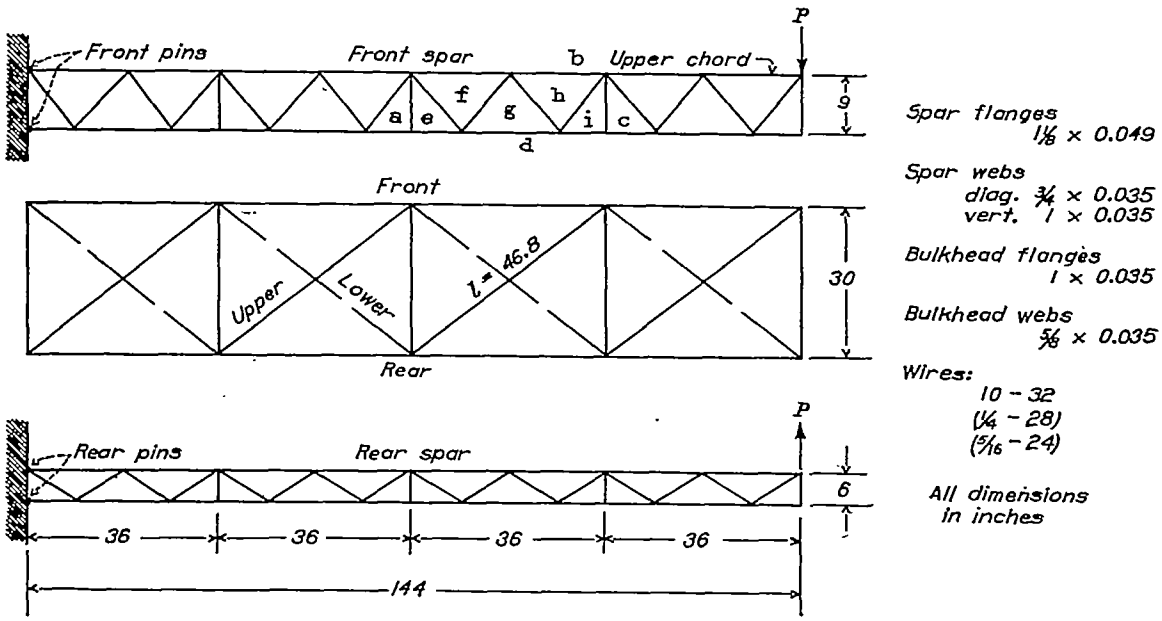

FIGURE 13.—Diagram of trussed wing frame.

The tests on the wing frame were made with three different sizes of wire: 10–32, ¼–28, and 5/16–24 and each with three different kinds of support: 4-pin support representing the support the frame would have in an actual airplane, 3-pin support at the wing root, and 2-pin support (one pin in front spar, one pin in rear spar). The latter methods of support eliminate the influence of the bending stiffness of the spars, so that the tests evaluate the properties of the frame as a pure torsion box.

The calculation of the bending and pure torsional stiffnesses of the frame is given in detail in the preceding calculation for case I, i.e., 10–32 wire. The pure torsional stiffnesses were calculated similarly for cases II and III, i.e., ¼–28 and 5/16–24 wire. With these values, the tip deflections were calculated by formula (8) for a 2-pin support (pure torsion box) and

a 4-pin support (wing frame). For the case of a 4-pin support, the deflections were also calculated by integrating the M/EI curves which checked the deflections obtained by the formula within 5 percent; the assumption of infinitely many ribs underlying the formula can therefore be used quite satisfactorily for as few as four ribs.

The comparison of test results and calculations showed that all computed deflections were much too large. The ratio of the calculated to the observed values was almost 2 (within less than 5 percent) in assumption of slack counterwires gave deflections 48 percent too high, whereas the assumption of taut counterwires gave deflections 26 percent too low for a 2-pin support.

This discrepancy may be explained as follows: If it is assumed that all counterwires were just about to go out of action at the highest test load used, the initial tensions must have been 48 percent, 36 percent, and 23 percent of the rated strength in cases I, II, and III, respectively. Obviously, the initial tension required for case I is rather high; it seems reasonable to assume

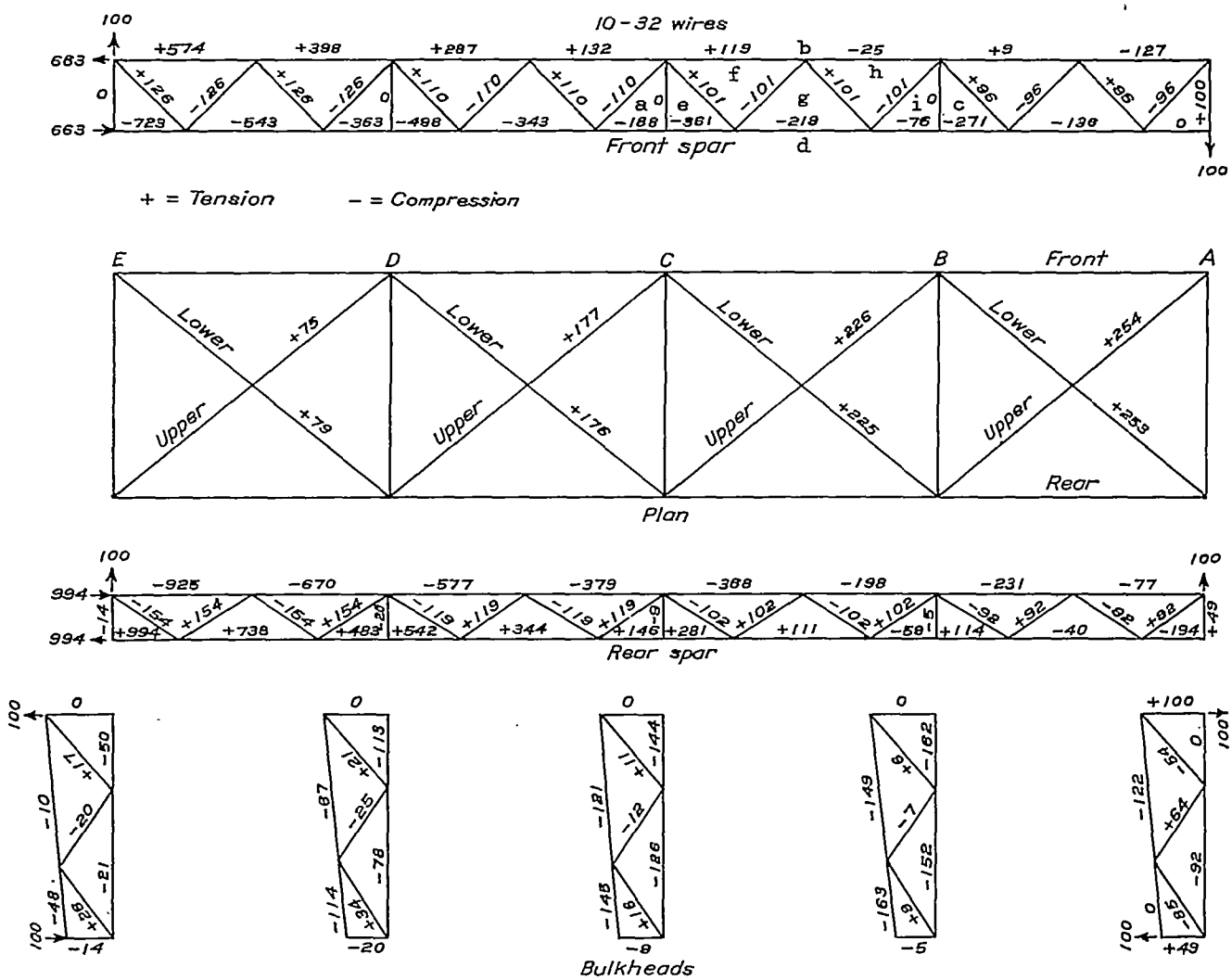

FIGURE 14.—Stress sheet for trussed wing frame (reference 9). Four-pin support; 100-lb. down on tip of front spar; 100-lb. up on tip of rear spar.

cases II and III for the 2-pin support. This relationship points to the possibility that the counterwires had sufficient initial tension to remain active throughout the test, in which case the pure torsional stiffness B_0 would be nearly doubled. The calculations were therefore repeated, using twice the original values of B_0. It was found that in cases II and III the calculated deflections for a 2-pin support were about 3 percent high and those for a 4-pin support about 9 percent low, errors which are well within the magnitude of errors possible either in calculation or in test. In case I the condition seemed to be in between: The that the actual initial tension was considerably less, so that the most highly stressed counterwires probably went out of action and reduced the pure torsional stiffness of the frame near the tip.

The test report makes no definite statements regarding the condition of the counterwires beyond recommending that in future tests they be omitted altogether. This recommendation probably indicates that their presence was felt to introduce uncertainties, to say the least. In view of this and other difficulties, such as questions on jig deflection, actual areas, and moduli of elasticity, the writer has made no more

concentrated effort to explain the differences between theory and experiment. The following conclusions may be drawn:

1. If an accurate check of the theory is desired, the initial tension of the wires must be known accurately. The easiest way to achieve this end is to remove the counterwires for test purposes.

2. In view of the fact that the tip deflection computed under the assumption of independent spars is about 4 times that observed for case I and about 10 times that for case III, the proposed method of calculation constitutes a vast improvement. The large percentage discrepancies left in some cases between theory and experiment can be explained by the uncertainty about the test conditions.

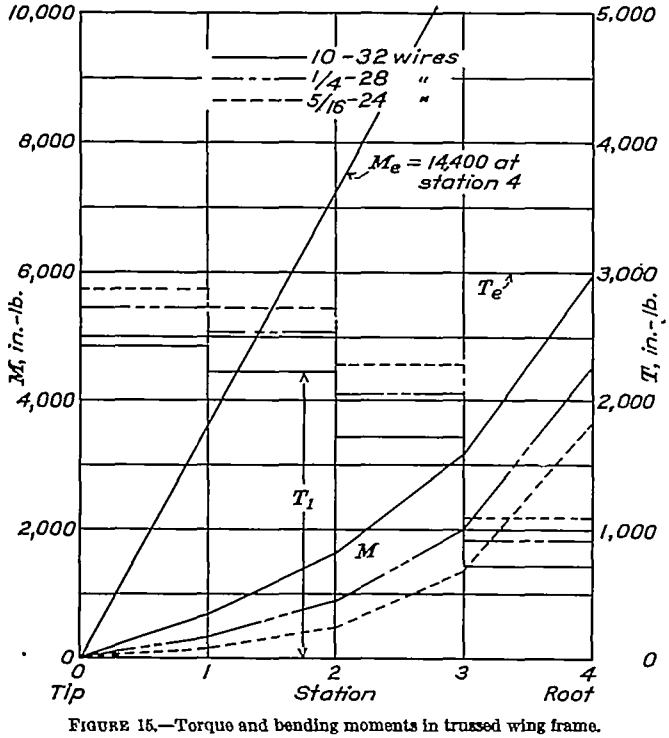

FIGURE 15.—Torque and bending moments in trussed wing frame.

3. The proposed method of calculation gives results equivalent to standard least-work calculations which treat the wing frame as a pin-jointed space framework while the labor is reduced to a point where the computations may be made as a routine design procedure. It may not be amiss to point out that design calculations—whether for stiffness or for strength—should be based on the assumption of all counterwires being slack, since this condition will ordinarily obtain under design loads.

Figure 15 shows the results of the calculations for the three tests with 10–32, ¼–28, and 5/16–24 wires.

EXAMPLES OF STRESSED-SKIN WINGS

As an example of stressed-skin wings, the bending moments and torsional deflections in an Atlantic C–2A Transport wing were calculated. The calculations for the relief moments are exactly analogous to those given in detail for the wire-braced wing frame, once the torsional stiffnesses have been calculated for each bay by formula (T–3) (appendix A).

The dimensions and properties of the wing frame and the test results are given in references 10 and 11; for the shear modulus, G=135,000 pounds per square inch was used (appendix B). The results of the calculations are shown in figures 16 and 17. The agreement between calculated and experimental twist is excellent.

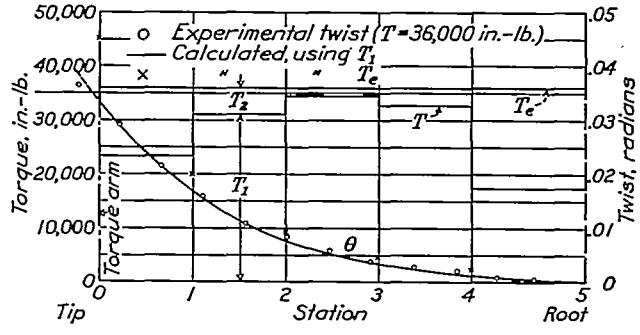

FIGURE 16.—Torque and twist in C–2A Transport wing.

The only test on a metal wing with parallel spars that has come to the attention of the writer is described in reference 12. The information given in the report is meager and contains some obvious errors. The conclusion may, however, be drawn that the calculated stiffness value is conservative.

WING FRAMES WITH NONPARALLEL SPARS

FRIEDRICHS-VON KÁRMÁN EQUATIONS FOR NONPARALLEL SPARS

Friedrichs and von Kármán indicate in their paper (reference 2) the possibility of deriving equations for

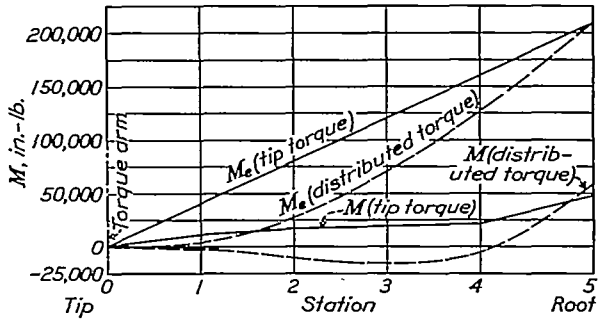

FIGURE 17.—Bending moments in C–2A Transport wing.

wing frames with nonparallel spars. The writer has made this derivation for the case of two spars having the same inclination with the transverse axis, but has found that the coefficients corresponding to p, q, r, s, and t (FK–13), contain so many terms that they are of no practical use. This unfortunate fact arises from two circumstances: First, both the bending moments and the torsional moments always have two components, since the coordinate system is not rectangular; second, cross products of bending stiffnesses and torsional stiffnesses arise, in a manner similar to the case of a beam with bending moments not in a principal

plane, where product-of-inertia terms arise in addition to moment-of-inertia terms. In view of the large range of proportions possible, it did not seem possible to derive any generally useful approximations of these equations for nonparallel spars, and it was necessary to resort to other methods of analysis.

APPROXIMATE METHODS OF CALCULATIONS

Good approximations for wings with small inclination of the spars may be obtained by assuming a constant spar spacing equal to the average spacing and using the Friedrichs-von Kármán equations. The actual spar spacing at any station is used, however, to compute the torsional stiffness at that station if the spar webs form two sides of the torsion box. This method was used by Friedrichs and von Kármán (reference 2) for calculating a duralumin test wing with a taper between spars of 1:2. The calculated angle of twist checks within about 5 percent, although

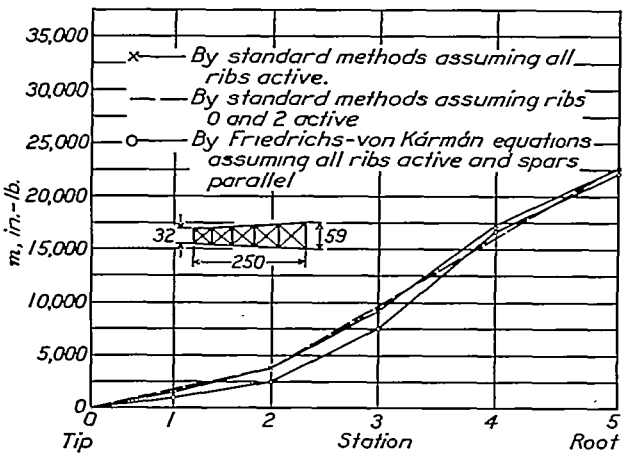

FIGURE 18.—Relief moments in XHB-3 wing frame calculated by three methods.

there is a discrepancy in the total deflections that indicates bending of the wing in addition to the twisting, in spite of the fact that the load applied was presumably a pure torque.

Another means of analyzing wing frames with nonparallel spars would be to use conventional methods, but to reduce the labor of computation by assuming that only two ribs are working; namely, the rib at the tip and a rib at one-third of the semispan from the tip, as previously explained.

In order to gain some idea of the relative results obtained with these different methods, they were applied to the wing frame described in reference 13. This frame, designated "XHB-3", had a semispan of 262 inches, and was sharply tapered in plan form and thickness. The spars were truss-type, of steel tubing, and the drag bracing consisted of wires that decreased in size from root to tip.

Figure 18 shows the relief moments for a load factor of 0.5 and the load distribution as used in the tests calculated by (1) the Friedrichs-von Kármán formulas, assuming constant spar spacing; (2) conventional methods, assuming all ribs working; and (3) conventional methods, assuming ribs 0 and 2 acting. Using method (2) as a basis of comparison, it will be seen that in this case method (3) gives a very close approximation for the bending moments in the spars. However, method (3) gives an incomplete picture of the shears in the spars and of the forces in the ribs; furthermore, it seems reasonable to assume on general principles that the probability of obtaining good approximations will usually be somewhat higher when method (1) is used than when method (3) is used. Method (1) is conservative compared with method (2) as shown on figure 18, and some comparative calculations on wings with constant-section spars indicate that it is always conservative in the practical range of stiffness ratios.

Figure 19 shows the comparison of external and internal bending moments for the XHB-3 wing, based

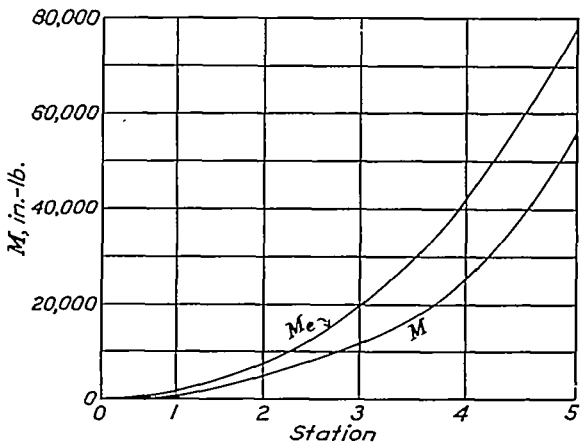

FIGURE 19.—Bending moments in XHB-3 wing frame.

on the Friedrichs-von Kármán results. By an integration of the resulting M/EI curve, the tip deflections were calculated for the unit torque acting on the wing, and the results used in combination with the calculated deflections for unit bending load to obtain the bending deflections at the tip in low and in high incidence.

In order to make a comparison with the experimental results it was necessary to consider the influence of the center section, since in these tests the fittings holding the spars at the root were not held by a rigid structure but were attached to the spars of a quite flexible center section corresponding to the actual condition in the airplane. It is obvious that the flexibility of the center-section spars will increase the bending deflections of the wing spars and, consequently, the amount of relief action. Some simple calculations for the case of only a tip rib acting showed that the relief moment at the root may be increased by about 33 percent for a wing with a torsional stiffness corresponding to that of the XHB-3 wing and a center section of propor-

tional length. The advantage over the wing built in at the root decreases quite rapidly, however, with increase of torsional stiffness and decrease of length of center section, so that it should be neglected entirely for ordinary design calculations.

The foregoing remarks should not be construed to mean that a flexible center section is desirable. The criterion for a good design is stiffness, not a large relief coefficient.

In the XHB–3 tests at high and low incidences, the direct bending deflections were always considerably larger than the bending deflections due to torque. Consequently, it was assumed as a first approximation that the relief action was not affected by the flexibility of the center section; however, the calculated deflections were compared not with the directly measured deflections but with the deflections measured from the tangent to the elastic curves of the spars at the hinge fittings. The direction of this tangent was calculated by assuming that the elastic curve was a circular arc over the center section, and the radius was calculated

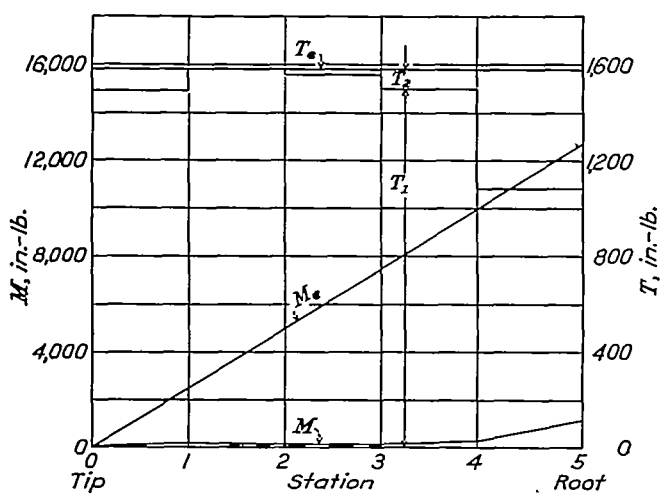

FIGURE 20.—Torque and bending moments in Driggs-Dart wing.

from the known deflections at the center line and at the hinge fittings. This method gave very consistent results for all tests and was therefore considered as satisfactory. The comparison between the results of this first approximation and the experimental results showed that the calculated deflections were 8 percent too high for both high and low incidences and both front and rear spars. In the second approximation—introducing a correction factor into the relieving effect—the differences for low incidence were reduced to 7 percent and 5 percent. The interaction being entirely neglected, the differences were increased to 10 percent low and 21 percent high for front and rear spars, respectively.

EXAMPLES OF STRESSED-SKIN WINGS WITH NONPARALLEL SPARS

An instructive example of high torsional stiffness is given by the Driggs-Dart wing (reference 14) which is a high-aspect-ratio wing for a very small single-seater airplane. It is covered with plywood of the same thickness as that used in the outboard half of the Atlantic C–2A Transport wing and has therefore a very high torsional stiffness and a very great amount of relief action. Figure 20 shows that the torque is carried almost entirely by the torsion tube, except near the root, and that the bending moment left in the spars is negligible except for a small amount at the root. Figure 21 shows the experimental and the calculated twist. The calculated twist was too large, which may be due partly to a higher shear modulus, partly to excess thickness of the plywood, and partly to neglecting the spars in the calculation of the pure torsional stiffness. Since the materials specifications permit 20 percent excess thickness, the calculated values of the twist were reduced by 20 percent and the resulting curve shows good agreement.

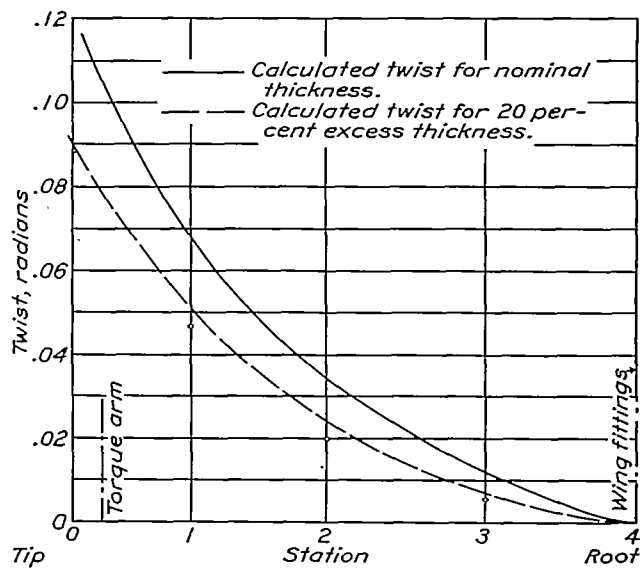

FIGURE 21.—Twist of Driggs-Dart wing.

A very interesting test on a plywood-covered wing is described in reference 15. The wing was tested under a distributed torque corresponding to the actual torque in a terminal-velocity dive. The bending moments along the span were measured at 17 stations by means of strain gages, and the torque T_2 carried by the spars was computed from these moments. Subtracting T_2 from the known external torque T_e gave the torque T_1 taken up by the torsion tube. Figure 22 shows the variation of T_e, T_1, and T_2 along the span, as well as the experimentally obtained bending moments M and the bending moments M_e which would exist without interaction.

It will be noted that for practical purposes the entire torque is carried by the torsion tube (skin) in the outer two-thirds of the semispan; farther inboard, the percentage of the total torque carried by the skin decreases rapidly. The curve of bending moments M is qualitatively similar to that calculated for the Atlantic C–2A wing shown in figure 17. Both curves show that, in the outboard portion of the wing, the

sign of the bending moment is opposite to that which would exist if the spars carried all the torque by bending. Quantitatively, however, the experimental bending-moment curve of figure 22 shows a much faster rise toward the root than does the calculated curve of figure 17. Unfortunately, it was not possible to calculate the relief moments because the bending properties of the spars were not given.

CONCLUDING REMARKS

A general idea of the theoretical magnitude of the relief action may be obtained from figure 23. This is a plot of the relief coefficient $C_R=m/M_e$ at the root against the "interaction coefficient" $C_i=\frac{B_0}{A_0}\frac{L^2}{b^2}$ for wing frames with constant-section spars. The relief coefficients were computed for three different types of

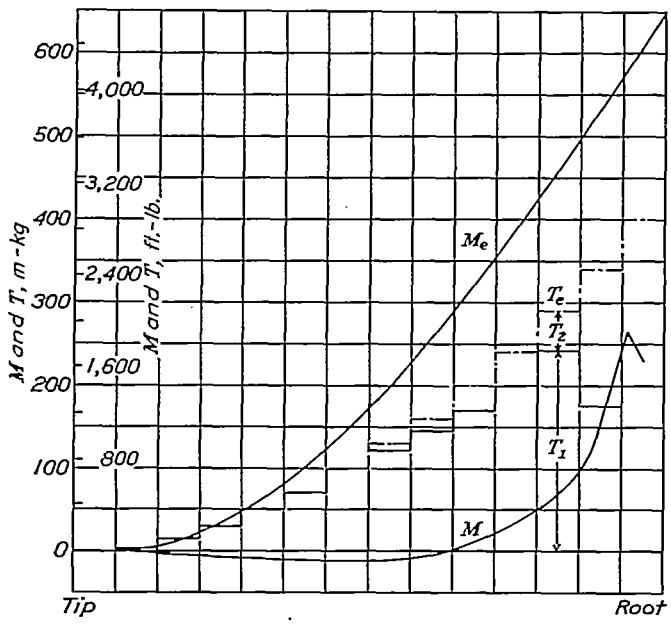

FIGURE 22.—Torque and bending moments (experimental) in plywood covered wing.

loading: namely, load concentrated at tip, load uniformly distributed along the span, and load tapered in the ratio of 2:1. Each type of loading was calculated for two types of interconnection between spars, a tip rib only, and an infinite number of ribs. It will be seen that the curves for the most important cases—uniform and tapered loads on wings with many ribs—lie very closely together, and that the relief action increases only very slowly for $C_i>30$, which is the stressed-skin range.

The calculated relief coefficients for the Driggs-Dart and the C–2A wings are also plotted on the figure, using the average value of B_0/A_0 along the span for computing the interaction coefficient. The points fall fairly close to the corresponding curves, although in both of these wings the bending stiffness as well as the torsional stiffness decreases rapidly as the tip is approached and the ratio B_0/A_0 varies irregularly along the span. This result suggests that for stressed-skin wings a good estimate of the theoretical relief action might be obtained without any calculation beyond that of the torsional and bending stiffnesses for a few stations.

Wings that owe their pure torsional stiffness to double drag-wire bracing or to the individual torsional stiffnesses of the spars, have, as a rule, $C_i<20$. In this range, reliable estimates of interaction on tapered wings cannot be obtained from figure 23, as the point for the XHB–3 frame indicates.

When the twist or, more important, the stresses under high loads are being calculated an extremely important fact must be borne in mind. The ordinary formulas for calculating bending and torsional stiffnesses only yield the so-called "initial stiffness", valid for small loads. Compact sections retain their initial stiffness until the stresses approach the limit

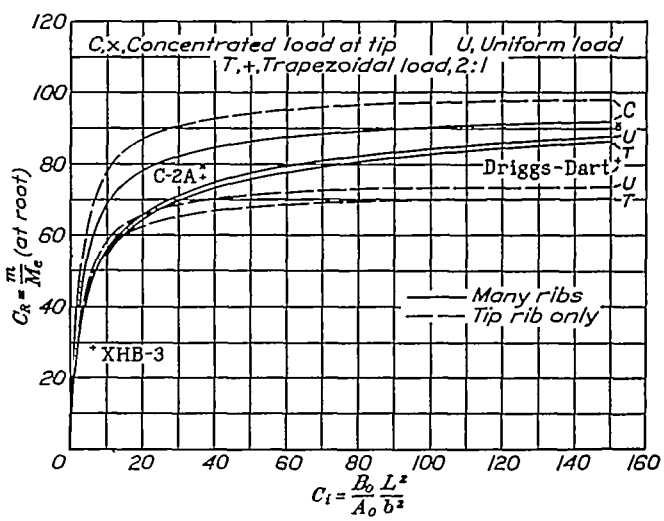

FIGURE 23.—Relief coefficient for wings with constant-section spars.

of proportionality, but the thin-walled sections now in common use suffer from an increasing loss of efficiency as the load increases, owing to the fact that parts of the structure buckle and no longer carry their share of the load. Since the rate of loss of efficiency with load will, in general, not be the same for the torsional stiffness as for the bending stiffness, the ratio B_0/A_0 will change with increase of load and, consequently, the amount of relief action will change.

In 2-spar wings covered with flat sheet the spars will quite often be of such a shape that they lose their bending stiffness at a slow rate, but the thin-walled torsion tube formed by the wing covering will lose its torsional stiffness rapidly, with a resulting decrease of interaction effect. The test results given in figure 22 may be cited as an example. The experimental value of the relief coefficient was somewhat less than 60 percent; it should be at least 70 percent, assuming $C_i=30$, which is about the minimum probable value.

If the stiffness of a structural member is a function of the load applied, the methods of analysis developed

in this paper, are, strictly speaking, inapplicable. However, if the load-deformation diagram of the member is known, a substitute member of constant stiffness may be defined by the condition that both the original and the substitute member must store the same amount of strain energy when a load is applied which increases from zero to the design load. A simple empirical method for estimating the torsional stiffness of thin shells under large torque loads has been published (reference 17).

Finally, the influence of torsionally stiff ribs might be touched upon. Throughout the present paper it was assumed that the ribs have no torsional stiffness. Under this assumption, a wing frame with constant-section spars connected by a tip rib rigid in bending will have a maximum relief coefficient of 0.75 when subjected to a uniformly distributed torque; the spar corresponds then to a cantilever beam supported at the free end. If the tip rib is now made rigid also in torsion, the relief coefficient increases to 0.83, the spar acting as a beam built in on both ends. The additional relief amounts to 0.08, or 11 percent of the original relief. Actually, only about half of this amount can be realized because the torsional stiffness of the rib is finite; the assumption of infinite stiffness in torsion is not generally permissible, unlike the case of bending stiffness.

With torsionally stiff spars, then, the additional relief due to ribs being stiff in torsion besides being stiff in bending is too small to justify the complication of the analysis. With spars weak in torsion, however, the relief due to ribs stiff in bending is small and the relief due to ribs stiff in torsion becomes relatively more important. The effect of torsionally stiff ribs on the twist of the wing frame is discussed in reference 18 for the case of spars with constant section.

LANGLEY MEMORIAL AERONAUTICAL LABORATORY,
NATIONAL ADVISORY COMMITTEE FOR AERONAUTICS,
LANGLEY FIELD, VA., *April 10, 1934.*

71040—30——6

APPENDIX A

FORMULAS FOR TORSIONAL STIFFNESS

For a rod of uniform cross section, built in at one end and twisted by a concentrated torque at the free end, the fundamental equation of torsion is

$$\theta=\frac{TL}{GJ}$$

Where θ, angle of twist at free end, radians.
T, torque.
L, length.
G, modulus of shear.
J, the torsion constant, a factor corresponding to the moment of inertia in the theory of bending. Analogous to the bending stiffness EI, the product GJ is termed the "torsional stiffness." Formulas for calculating the torsion constant for various sections are given below.

CIRCULAR TUBE

$$J=I_p$$

where I_p is the polar moment of inertia.

RECTANGLE

(Fig. 24a)

$$J=\frac{1}{3}bc^3\left[1-0.630\frac{c}{b}+0.052\left(\frac{c}{b}\right)^5\right] \qquad \text{(T-1)}$$

I-BEAM

(Fig. 24b)

$$J=2J_1+J_2+2\alpha D^4 \qquad \text{(T-2)}$$

where $J_1=J$ of flange $=\frac{1}{3}\times b_1c_1^3\left(1-0.630\frac{c_1}{b_1}+0.052\left(\frac{c_1}{b_1}\right)^5\right)$

$J_2=J$ of web $=\frac{1}{3}b_2c_2^3$ (see reference 16).

D, diameter of circle inscribed at juncture.
α, constant from reference 16. The value of α varies between 0 and 0.3 for usual proportions. If the radius of the fillet is zero, α varies from 0 for $c_2=0$ to $\alpha=0.15$ for $c_2=c_1$.

THIN-WALLED TUBE

(Fig. 24c)

$$J_0=\frac{4A^2}{\int\frac{ds}{t}} \qquad \text{(T-3)}$$

where A, area enclosed by median line.
ds, differential element of perimeter.
t, wall thickness of ds.

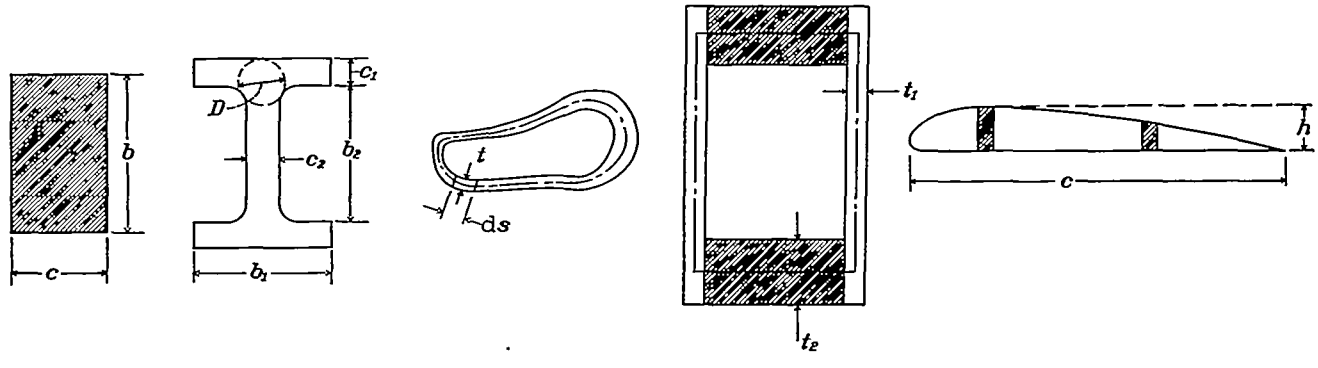

FIGURE 24.

The integral is taken around the whole perimeter. The shearing stress at any point is

$$f_s=\frac{T}{2At}$$

The shearing force per inch of perimeter is

$$f_st=\frac{T}{2A}$$

WOODEN BOX BEAM

(Fig. 24d)

The torsional stiffness is the sum of the torsional stiffness of the beam considered as a thin-walled tube (using the median line as perimeter) and of the individual stiffnesses of the flanges. (See reference 15.)

$$GJ=G_pJ_0+2G_FJ_F \qquad \text{(T-4)}$$

where G_p, shearing modulus of plywood.
G_F, shearing modulus of solid wood in flange.
J_F, J of flange (by formula (T–1)).
When computing J_0, the thickness t_F must be replaced by an effective thickness, which is expressed by

$$t_F'=t_F\times\frac{G_F}{G_p}$$

METAL BOX BEAM

In this case formula (T–3) is used, but if the web has lightening holes, a reduced effective thickness must be used. If the holes are cut so that the remaining web forms a truss, the calculation is similar to that given for wire drag bracing in the main text. If the lightening holes are of any other shape, tests must be made, since no rules are at present available. The reduction in thickness is not proportional to the reduction in web area, but is much higher. Reducing the web area 50 percent by means of round lightening holes reduced the effective thickness to 7 percent of the actual value in one case.

WING SECTION WITH STRESSED SKIN

(Fig. 24e)

$$GJ=G_0J_0+(GJ)_F+(GJ)_R$$

where G_0, shearing modulus of cover material.
J_0, J of whole wing section.
$(GJ)_F$, torsional stiffness of front spar.
$(GJ)_R$, torsional stiffness of rear spar.
The two spar stiffnesses are usually very small compared with G_0J_0. For the computation of J_0 it is useful to remember that

$$A=k\times h\times c$$

where k usually lies between 0.65 and 0.71.

The formula given for GJ neglects the fact that the spars act also as inner walls of the torsion tube. This effect can be taken into account by deriving a more accurate formula with the help of the membrane analogy or the hydrodynamic analogy for torsion. The result by the simple formula given above is usually not more than 5 percent in error and is conservative.

NUMERICAL EXAMPLES OF THREE TYPES OF BEAMS

(Fig. 25)

Material: Spruce
Webs of box beam: 2-ply, 45° spruce
$E=1.3\times10^6$ lb./sq. in.
$G=84{,}000$ lb./sq. in. for solid spruce
$G=420{,}000$ lb./sq. in. for 45° plywood

Type of beam	$A=EI$ lb. in.^{2}	$B=GJ$ lb. in.^{2}	$A/B=EI/GJ$
I-beam	75,700,000	105,000	720.0
Solid beam	73,300,000	465,000	158.0
Box beam	71,000,000	2,876,000	24.7

CALCULATION OF B

Rectangular spar (formula (T–1))

$$J=\frac{1}{3}\times1.323^3\times8\left(1-0.63\,\frac{1.323}{8}\right)=5.54\text{ in.}^4$$
$$B=GJ=465{,}000\text{ lb.in.}^2$$

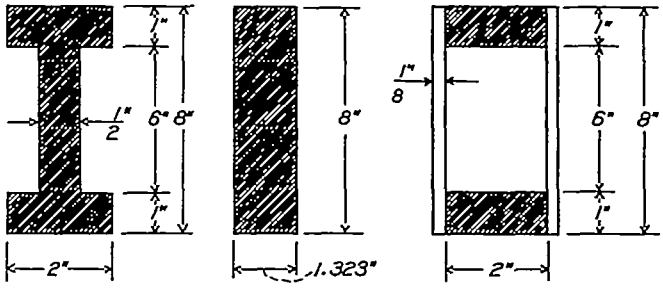

FIGURE 25.

Routed spar (formula (T–2))

$$J=2\times\frac{1}{3}\times2\times1^3\left(1-0.63\times\frac{1}{2}\right)+\frac{1}{3}\times6\times\left(\frac{1}{2}\right)^3$$
$$+2\times0.035\times1.06^4=1.251\text{ in.}^4$$
$$B=GJ=105{,}000\text{ lb.in.}^2$$

Box spar (formula (T–4))

$$A=7\times2.125=14.875\text{ sq.in.}$$

For calculating J_0, the effective thickness of the flanges is

$$t'=1\times\frac{84{,}000}{420{,}000}=0.200$$

therefore

$$J_0=\frac{4\times14.875^2}{\frac{14}{0.125}+\frac{4.12}{0.200}}=6.65\text{ in.}^4$$

$$2J_1=2\times\frac{1}{3}\times2\times1^3\left(1-0.63\times\frac{1}{2}\right)=0.913\text{ in.}^4$$

$$G_pJ_0=420{,}000\times6.65=2{,}800{,}000$$
$$2G_FJ_F=84{,}000\times0.913=\quad76{,}000$$
$$GJ=G_pJ_0+2G_FJ_F=2{,}876{,}000\text{ lb.in.}^2$$

APPENDIX B

MODULI OF ELASTICITY

Material	Young's modulus [1]		Shearing modulus G		Reference
	E_C (design)	E_T (true)			
Duralumin	10×10^6		4×10^6		F.P.L. tests.
Spruce, solid	1.3×10^6	1.413×10^6	84×10^3		
			Plywood		
			45°	Parallel-perpendicular	
Spruce	1.3×10^6	1.413×10^6	420,000		Do.
Poplar	1.3×10^6	1.413×10^6	335,000	99,000	Do.
Birch	1.78×10^6	1.935×10^6	483,000	135,000	(?)
Birch [3]	1.535×10^6		640,000	142,000	Reference 15.

[1] The values for E_C and E_T are Forest Products Laboratory values and have been published in several handbooks.
[2] From values for poplar, assuming proportionality to Young's modull E.
[3] From a very extensive series of tests on spars and wings at the D.V.L. (Germany). The birch is evidently not quite the same as American birch.

As a general rule, the Forest Products Laboratory recommends 45° plywood: $G=\frac{E_T}{5}=\frac{E_C}{4.5}$. Parallel-perpendicular plywood: $G=\frac{E_T}{16}=\frac{E_C}{14.5}$. Values resulting from the application of this rule are low compared with the values given in the table. The tabulated values were used in the present paper as representing the most probable values for the purpose of checking tests by theory.

LIST OF IMPORTANT SYMBOLS

E, modulus of elasticity.
G, modulus of shear.
I, moment of inertia.
J, torsion constant.
$A=EI$, bending stiffness of a member.
$B=GJ$, torsional stiffness of a member.
A_0, see equation (2) of text.
B_0, see equation (5) of text.
b, distance between spars.
L, length of spar.
l, length of bay between ribs.
S, shear.
M_s, bending moment due to external loads (equal to the bending moment that would exist in spars if ribs were cut).
m, relief bending moments in a spar due to ribs transferring loads from other spar.
M, final bending moment in spar.
T_1, part of total torque carried by torsional shearing stresses in torsion tube.
T_2, part of total torque carried by bending of spars.

REFERENCES

1. Ballenstedt, L.: Influence of Ribs on Strength of Spars. T.N. No. 139, N.A.C.A., 1923.
   The numerical solution of a representative case with uniform-section spars.
2. Friedrichs, K., and von Kármán, Th.: Zur Berechnung freitragender Fluegel. Abhandlungen aus dem Aerodynamischen Institut der Technischen Hochschule Aachen. Heft 9 (1930).
   The derivation of the Friedrichs-von Kármán equation. The second test of reference 8 is briefly referred to.
3. Fradiss, Jean, and Thieblot, Armand: Analysis of the Wing and Other Indeterminate Structures. Aviation, July 20, 1929, pp. 195–202, and Sept. 21, 1929, pp. 644–645.
4. Kartveli, Alexander, and Chagniard, Edmund: Analysis of Torsional Stresses in Airplane Wings. Aviation Engineering, June 1929, pp. 7–14.
5. Thalau, K.: Computation of Cantilever Airplane Wings. T.M. No. 325, N.A.C.A., 1925; Calculation of Combining Effects in the Structure of Airplane Wings. T.M. No. 366, N.A.C.A., 1926; Über die Verbundwirkung von Rippen im freitragenden, zweiholmigen, und verspannungslosen Flugzengflügel. Z.F.M., Oct. 28, 1925, pp. 415–444.
   Formulas for various cases with tip rib only. Series of calculations, varying number and position of ribs.
6. Gabrielli, Giuseppe: Torsional Rigidity of Cantilever Wings with Constant Spar and Rib Sections. T.M. No. 520, N.A.C.A., 1929.
   Solution by integration of differential equation for wing with infinitely many ribs.
7. Luczynski, Z.: Etudes Experimentales sur la Cooperation des Longerons dans les Ailes en Porte à Faux. Bull. No. 8, Institute des Recherches de L'Aeronautique, Warsaw, Poland, 1932, pp. 83–129.
   Measurements of deflection curves and strains in spars of simple wing frames.
8. von Fákla, Stefan: Biegungs- und Torsions-steifigkeit des freitragenden Flügels. Luftfahrtforschung 4.Band, Heft 1, June 5, 1929, pp. 30–40.
   Measurements of deflection curves of model wooden wing frame and full-size duralumin-wing frame.
9. Bailey, N. R.: Progress Report on the Study of Torsion on Wing Framework. A.C.I.C. No. 584, Matériel Division, Army Air Corps, 1927.
   Deflection measurements on tubular truss wing frame. Discussion of least-work analysis and approximate methods of analysis.
10. Spere, Charles J.: Determination of the Elastic Axis and Natural Periods of Vibration of the Atlantic C–2A Monoplane Wing. A.C.I.C. No. 645, Matériel Division, Army Air Corps, 1930.

11. Carpenter, Stanley R.: The Calculation of the Natural Frequency of a Cantilever Monoplane Wing. A.C.I.C No. 649, Matériel Division, Army Air Corps, 1930.
12. Pegna, G., and Gabrielli, G.: Esperienze sul contributo della coppertura sulla rigidezza a torsione delle ali. L'Aerotecnica, November 1928, pp. 885–895.
Experimental results on torsion test of stressed-skin wing and component parts.
13. Weaver, Edgar R.: Static Test of the XHB–3 Experimental Two-Spar Wing Structure Built by the Keystone Aircraft Corporation. A.C.I.C. No. 616, Matériel Division, Army Air Corps, 1928.
14. Brown, C. G.: Static Test of Matériel Division 27-Foot Metal Cantilever Wing and Driggs Dart 27-Foot Wood Cantilever Wings. Technical Report 3415, Matériel Division, Army Air Corps, 1931.
15. Hertel, Heinrich: Die Verdrehsteifigkeit und Verdrehfestigkeit von Flugzeugbauteilen. D.V.L. Yearbook, 1931, pp. 165–220.
Very extensive series of tests on torsional stiffness and strength of wooden box beams and wings, single spar and 2-spar, wood and metal.
16. Trayer, George W., and March, H. W.: The Torsion of Members Having Sections Common in Aircraft Construction. T.R. No. 334, N.A.C.A., 1930.
17. Kuhn, Paul: The Torsional Stiffness of Thin Duralumin Shells Subjected to Large Torques. T.N. No. 500, N.A.C.A., 1934.
18. Cox, H. Roxbee, and Williams, D.: Effect of Stiff Ribs on Torsional Stiffness of Wings. R. & M. No. 1536, British A.R.C., 1933.